EVALUATION OF POWER SYSTEM SECURITY AND DEVELOPMENT OF TRANSMISSION PRICING METHOD

A Dissertation

by

HYUNGCHUL KIM

Submitted to the Office of Graduate Studies of
Texas A&M University
in partial fulfillment of the requirements for the degree of

DOCTOR OF PHILOSOPHY

August 2003

Major Subject: Electrical Engineering

EVALUATION OF POWER SYSTEM SECURITY AND

DEVELOPMENT OF TRANSMISSION PRICING METHOD

A Dissertation

by

HYUNGCHUL KIM

Submitted to Texas A&M University
in partial fulfillment of the requirements
for the degree of

DOCTOR OF PHILOSOPHY

Approved as to style and content by:

Chanan Singh (Chair of Committee)	
Ali Abur (Member)	Garng M. Huang (Member)
Bani K. Mallick (Member)	Chanan Singh (Head of Department)

August 2003

Major Subject: Electrical Engineering

ABSTRACT

Evaluation of Power System Security and
Development of Transmission Pricing Method. (August 2003)
Hyungchul Kim, B.S., Korea University;
M.S., Korea University
Chair of Advisory Committee: Dr. Chanan Singh

The electric power utility industry is presently undergoing a change towards the deregulated environment. This has resulted in unbundling of generation, transmission and distribution services. The introduction of competition into unbundled electricity services may lead system operation closer to its security boundaries resulting in smaller operating safety margins. The competitive environment is expected to lead to lower price rates for customers and higher efficiency for power suppliers in the long run. Under this deregulated environment, security assessment and pricing of transmission services have become important issues in power systems. This dissertation provides new methods for power system security assessment and transmission pricing.

In power system security assessment, the following issues are discussed 1) The description of probabilistic methods for power system security assessment 2) The computation time of simulation methods 3) on-line security assessment for operation. A probabilistic method using Monte-Carlo simulation is proposed for power system security assessment. This method takes into account dynamic and static effects corresponding to contingencies. Two different Kohonen networks, Self-Organizing Maps and Learning Vector Quantization, are employed to speed up the probabilistic method. The combination of Kohonen networks and Monte-Carlo simulation can reduce computation time in comparison with straight Monte-Carlo simulation. A technique for security assessment employing Bayes classifier is also proposed. This method can be useful for system operators to make security decisions during on-line power system operation.

This dissertation also suggests an approach for allocating transmission transaction costs based on reliability benefits in transmission services. The proposed method shows the transmission transaction cost of reliability benefits when transmission line capacities are considered. The ratio between allocation by transmission line capacity-use and allocation by reliability benefits is computed using the probability of system failure.

To my wife and my parents

ACKNOWLEDGEMENTS

This is a great opportunity to express my thanks to people and organizations that have helped me complete this dissertation.

First, I have no words to express my most sincere gratitude to my graduate studies advisor, Dr. Chanan Singh for his knowledge and support during my doctoral studies at Texas A&M University. Without his advice, guidance, and encouragement, the research for this dissertation would have been impossible. I am deeply grateful to him for his help and suggestions, not only in academics, but also in my personal life. I also convey my thanks to the members of my graduate studies committee, Dr. Ali Abur, Dr. Garng M. Huang, Dr. Bani K. Mallick, and the Graduate Council Representative Dr. Maynard Bratlien who have helped me throughout my doctoral program.

Texas Advanced Technology Program and the NSF(National Science Foundation) Grant ECS-9903747 also deserve my thanks. I would like to thank Ms. Lisa Lister and Ms. Tammy Carda for their help during my graduate studies. I wish to acknowledge the Electrical Engineering Department of Texas A&M University for giving me excellent academic opportunities. I gratefully acknowledge the support from the Ministry of Commerce, Industry and Energy, and Korea Electric Power Research Institute.

Sincere thanks and gratitute are extented to Professor Sae-Hyuk Kwon, who was my advisor during my graduate studies at Korea University. I appreciate his constant encouragement throughout my studies at Texas A&M University.

I also want to express my gratitude to the people who worked closely with me. My thanks go to Yan Ou, Samaan Nader, Xingbin Yu, Nirmal-Kumar C Nair, Yishan Li, and Ping Yan.

Special thanks go to my dear parents and parents-in-law. Their unconditional love has been with me throughout my life. I owe them a debt that can never be repaid.

Finally, I offer my deepest thanks to my wife Se Jung and my lovely sons Donghyun and Dongha.

TABLE OF CONTENTS

Page

CHAPTER Page

CHAPTER Page

LIST OF FIGURES

FIGURE Page

LIST OF TABLES

TABLE Page

CHAPTER I

INTRODUCTION

A. Introduction

Since its inception, the electric power industry in many countries around the world operated in the vertically integrated environment. There was only one company or government agency that generated, delivered and distributed electric power.

In 1978, PURPA (Power Utility Regulatory Policies Act) was enacted that requires utilities to purchase power from QFs (Qualifying Facilities), which are basically non-utility generators. The United States Congress signed EPAct (Energy Policy Act) in 1992, which authorized FERC (Federal Energy Regulatory Committee) to order utility companies to allow non-utility producers in wholesale markets open access to their transmission lines. In 1996, FERC issued Order 888 and Order 889 that mandated electric utilities to open up the transmission systems on an equal basis. Order 888 orders all utilities to offer nondiscriminatory open access and ancillary services. Order 889 provides an equal access for all by OASIS (Open Access Same-time Information System) and Standard of Conduct.

With the advent of competition, one of the primary consequences under deregulated environment is the effect on power system reliability. Now, many utility companies are operating a system with high security margin in power system reliability. According to the report [1], deregulation may greatly increase power transfers and degrade power system reliability. The impact of deregulation influences reliability evaluation for power system planning and operation.

This dissertation follows the style and format of *IEEE Transactions on Power Systems.*

B. Research Objectives and Organization of Dissertation

This research is focused on security assessment and the development of transmission pricing methods in power systems. The research objectives are given below. The first three objectives deal with security assessment and the last one relates to a transmission pricing method.

- The first objective is the development of probabilistic security methods involving dynamic aspects in power system reliability. Power system security assessment is composed of both steady state (static) and dynamic security analysis. Since dynamic effects are important in security assessment, these cannot be ignored in the development of a probabilistic security method. The evaluation of security breach for a certain contingency requires transient stability studies, the satisfaction of load without violation of constraints and voltage stability studies. A probabilistic method provides useful information about the possibility of system security for operational and facility planning.
- The second objective is to develop techniques for power system security assessment by combining Monte-Carlo simulation and Kohonen networks. The objective here is to overcome the problem of large amount of computation time required for straight Monte-Carlo simulation. This method also takes into account dynamic and steady state effects including transient stability and voltage stability. The use of straight Monte-Carlo simulation for reliability security analysis has a disadvantage that the evaluation of security breach for each sampled status is time consuming. Data classification by Kohonen networks can reduce sampling data, which reduces computation time for reliability security indices when using classified data. Kohonen networks can be classified by learning types: SOM (Self-Organizing Maps) and LVQ (Learning Vector Quantization). Two different approaches are implemented in this dissertation for power system reliability evaluation: SOM-MCS (The combination of Self-Organizing Maps and Monte-Carlo simulation) and LVQ-MCS (The combination of Learning Vector Quantization and Monte-Carlo simulation). The

efficiency of SOM-MCS and LVQ-MCS approaches will be demonstrated respectively.

- The third objective is to develop a technique using a Bayes classifier for static security assessment in power systems. The Bayes classifier provides a method to evaluate security breach without a complicated contingency analysis and can reduce the computational burden. Security status of a given feature vector is determined by maximum value of Bayes decision function. The case study of the WSCC system is presented to demonstrate the efficiency of this approach.
- The fourth objective is to develop a new approach for allocating transmission transaction costs based on reliability benefits in transmission services. Transmission embedded costs, which allocate transmission transaction costs, should be considered not only by allocation based on transmission line capacity-use but also by allocation based on reliability benefits. The transmission line capacity in an actual power system plays an important role in assuring system reliability.

Chapter II provides the literature review of techniques for power system reliability evaluation and transmission pricing methods. In the description of power system security studies, deterministic methods and probabilistic methods are described. Embedded cost methodologies and incremental cost methodologies are also explained in transmission pricing methods. Chapter III deals with the first objective, modeling of probabilistic security. It contains transient stability studies, optimal power flow for minimization of load shedding, and voltage stability studies. Chapter IV relates to the second objective, power system security assessment by combining Monte-Carlo simulation and Kohonen networks. Chapter IV develops an algorithm for power system security evaluation using Self-Organizing Map (SOM) combined with Monte-Carlo simulation. Also, it introduces the algorithm of Learning Vector Quantization (LVQ) combined with Monte-Carlo simulation for power system security evaluation. In Chapter V, a method for security assessment employing a Bayes classifier is proposed. This method can be useful for system operators to make security decisions in on-line power system operation. Chapter

VI deals with pricing methods for transmission services. Finally, Chapter VII gives the summary of this dissertation and reviews of the significance of this research. It also suggests future research topics.

CHAPTER II

REVIEW

A. Power System Reliability

The primary role of a power system is to provide reliable and continuous electrical energy to satisfy system load. Power system reliability, in a broad sense, can be defined as the ability of the system to provide an adequate supply of electric power with satisfactory quality. Power systems have three main components: generation, transmission and distribution systems. The generation systems generate electricity and transmission systems deliver the generated electricity to distribution systems for supplying load. The generation systems together with transmission systems are usually called the composite system or the bulk power system.

The reliability of a composite power system is comprised of both adequacy and security assessments [2-4]. Adequacy assessment relates to the ability of the system to supply energy requirements of customers in a satisfactory manner. Since adequacy assessment deals with static condition, it does not include the evaluation of the system response to transient disturbances. Security assessment deals with the ability of the electric systems to survive sudden disturbances such as electric short circuits or unanticipated loss of system elements. This includes the response of the system caused by the loss of generations and transmission lines.

The typical indices used in power system reliability evaluation are the following

- *Loss of Load probability* (LOLP) is the probability that some portion of load demands may not be satisfied by the available generating capacity under the specified operating conditions and policies. LOLP is currently the most widely used reliability index. *Loss of Load Expectation* (LOLE) is the expected period of time during a given period, in which the daily peak load is expected to exceed the available generating capacity. The LOLE in *h/y* can be obtained by multiplying the LOLP by 8760 hours. LOLP and LOLE are often used interchangeably.

- *Loss of Load Frequency* (LOLF) is the expected number of occurrence during a given period of time that the system may fail to meet its load demand.
- *Expected Unserved Energy* (EUE) is the expected amount of energy during a given period of time that the system may be unable to supply to the consumers due to the loss of generation or load uncertainty. Typical unit is MW*h/year*.

B. Power System Security Studies

In the past, reliability analysis has focused primarily on adequacy assessment. Power system security assessment, however, becomes an important issue for planning and operating power systems under deregulated environment. In a more competitive environment, security assessment should be done in a more realistic manner so that the investment of resources can be accomplished in a cost-effective manner. Generally, there are two fundamental approaches in a security study. The first is the deterministic criterion and the second is the probabilistic criterion.

1. Deterministic Criterion

To maintain system reliability, most utilities use deterministic criterion [5, 6] with a safety margin to cover all uncertainties such as an overload, voltage collapse and transmission line faults. The deterministic criterion indicates whether a system is secure during certain outages. The calculation of this criterion is simple and requires little data. However, it cannot directly indicate system reliability and does not reflect likelihood of component failures.

The procedure for deterministic criterion is as follows.

- Select the initial load condition, generation dispatch, and network topology that is a base case model of operational planning of the system.
- Select contingency set.
  - Type of fault
  - Location of fault
  - Faulted element and the switching time

- Evaluate system response and identify violation of the performance criteria.
- Identify the most serious contingency and the limit for each critical parameter.

2. Probabilistic Criterion

The electric power utility industry is undergoing a tremendous change in the deregulated environment. Since the introduction of competition leads system operation closer to its limits, the deterministic criterion may not result in efficient utilization of resources. Probabilistic criterion can recognize the probabilistic nature of system components. These methods fall into two broad categories: analytical methods and Monte-Carlo simulation methods.

- Analytical methods [3, 4, 7, 8] are based explicitly or implicitly on contingency enumeration and compute reliability indices by using mathematical solutions. Once the contingencies are selected, the evaluation of security breach under given conditions is carried out by using a suitable flow and stability calculation technique until all the selected contingencies have been evaluated. The advantage of analytical methods is that accurate results can be obtained if all the states in the state space can be enumerated and evaluated. The application of probabilistic criterion using the analytical methods in security assessment has already received some attention [9 - 11]. Analytical methods based on conditional probability, however, require intensive computation effort when applied to a system with many components.
- Monte-Carlo simulation methods [12] obtain the result by collecting and analyzing sample data based on statistical experiments. There are two basic approaches for Monte-Carlo simulation, sequential simulation and non-sequential simulation. In non-sequential simulation also called random sampling, a system state can be determined by random sampling based on the probability distributions of the component states regardless of sequences of occurrence. It is difficult to compute the index of frequency using this approach. The sequential simulation is based on component state duration. It proceeds by generating a sequence of events using random numbers and probability distributions of random variables. Further, there are

two methods in sequential Monte-Carlo simulation, the fixed interval method and the next event method. In the fixed interval method, system states are updated with a fixed interval. In a next event method, system states are updated at the occurrence of an event. Monte-Carlo simulation is suitable for analysis of complicated systems such as a power system, but it also requires large amount of computation time to achieve satisfactory statistical convergence and the characterization of repeated sampling states in security assessment.

C. Transmission Pricing Methods

In deregulated environment, the introduction of competition is expected to achieve lower rates for customers and higher efficiency for power suppliers in the long run. Pricing transmission services then plays a crucial role in a competitive market.

To calculate the actual cost of transmission services is not an easy task. The cost of transmission services should be economically equitable to consumers as well as power suppliers. Electric utility companies need to know the actual cost in order to decide on various types of services correctly. The price in transmission services is determined by the sum of the embedded costs and incremental cost. Embedded cost methodologies or incremental cost methodologies can compute the cost of transmission line capacity-use separately. Some methodologies can also be implemented with embedded cost methodology and incremental cost methodology together. Pricing methods are discussed as follows.

1. Embedded Cost Methodologies

Embedded costs, used by the utility industry, allocate existing transmission facilities to the transmission wheeling transaction. The costs occurred by new transactions are first summed up and are then allocated. The embedded cost methodologies include postage stamp methodology, contract path methodology, distance based MW-mile methodology and power flow based MW-mile methodology [13].

- A *"postage stamp"* methodology sets a price on use of the grid that depends only on amount of power, the duration of use. Like mailing a letter, customers pay the same amount regardless of distance or location of transmission usage. Simplicity is the strong selling point, but it ignores the actual system operation.
- A *"contract path"* methodology is based on the cost of a single identified path. In spite of many parallel paths, customers pay on the basis of one transmission line. This methodology is simple but it can get a system operator into trouble by overloading the grid.
- A *"distance based MW-mile"* methodology is a wholesale wheeling price proportional to both amount and distance. This methodology is simple to apply to a real power but it can cause transmission congestion problems.
- A *"power flow based MW-mile"* methodology allocates the charges for each wheeling participant based on the use of existing transmission facilities. It is simple to understand and to apply to real power systems. Capacity-use is determined by the amount of power transmitted and transmission line length.

2. Incremental Cost Methodologies

Incremental cost methodologies [14-15] require only the new transmission transaction costs caused by the new customers. Two major viewpoints related to incremental cost methodologies are short run/long run and incremental/marginal costs. Incremental cost approach is carried out by comparing the transmission costs with and without the transaction while marginal costs approach would multiply the cost for unit of additional transaction by the size of that transaction. Therefore, these methodologies include short-run incremental costs (SRIC), long-run incremental costs (LRIC), short-run marginal costs (SRMC) and long-run marginal costs (LRMC).

CHAPTER III

MONTE-CARLO SIMULATON METHOD IN PROBABILISTIC SECURITY ANALYSIS

A. Problem Formulation

The security analysis relates to the ability of the electric power systems to survive sudden disturbances such as electric short circuits or unanticipated loss of system elements. It consists of both steady state and dynamic security analyses, which are not two separate issues but should be considered together. In steady state security analysis including voltage security analysis, the analysis checks that the system is operated within security limits by OPF (optimal power flow) after the transition to a new operating point. Until now, many utilities have difficulty in including dynamic aspects due to computational capabilities. On the other hand, dynamic security analysis is needed to ensure that the transition may lead to an acceptable operating condition. Transient stability, which is the ability of power systems to maintain synchronism when subjected to a large disturbance, is a principal component in dynamic security analysis. Usually any loss of synchronism may cause additional outages and make the present steady state analysis of the post-contingency condition inadequate for unstable cases. This is the reason for the need of dynamic studies in power systems.

Probabilistic criterion can be used to recognize the probabilistic nature of system components while considering system security. In this approach, we do not have to assign any predetermined margin of safety. A comprehensive conceptual framework for probabilistic static and dynamic assessment is presented in this chapter. The simulation results of the Western System Coordinating Council (WSCC) system compare an analytical method with Monte-Carlo simulation (MCS). Also, a case study of the extended IEEE Reliability Test System (RTS) shows the efficiency of this approach.

B. System Model in Power System Security Analysis

1. System Operating State

The system operating states, which provide a conceptual basis for making security decisions in operational and long term planning, can be divided into normal, alert, and emergency states for security evaluation of composite systems [16,17] as shown in Fig. 1.

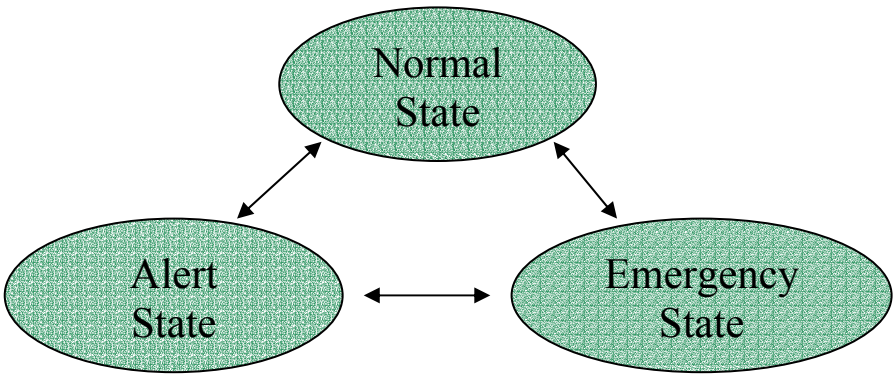

Fig. 1. System Operating State

In the normal state, all equipment and operation constraints are within their limits. The system can tolerate an assumed contingency without violating limits. As expected, the system including generators, transmission lines and loads has no difficulty. The alert state is similar to a normal state in that all constraints are satisfied. However, when a contingency occurs, sufficient margin is no longer available. In emergency state, the system may violate the equipment and operating constraints, and load may be curtailed. Compared with loss of load probability (LOLP) in adequacy studies, the probability of emergency state includes probabilities of voltage instability and transient instability. Operating constraints are within limits both in normal and alert state. The probability of emergency state can be expressed as the complement of the sum of these two state probabilities.

2. Security Constraints and Mathematical Modeling

Sudden disturbances of a power system may result from weather, environment, generation failure or human error. Transmission lines, with greater exposure to the changes of weather than generators, are one of the important sources of system disturbance. When a sampled contingency is a transmission line fault, transient stability analysis is performed first. Sudden loss of a transmission line can generate transient instability, transmission overloads and voltage drops. Therefore, security assessment in power systems requires analyzing transient behavior as well as evaluation of post contingency steady state. Steady-state constraints require the system to supply load without violating operating conditions and load curtailment. On the other hand, transient state constraints require the system to remain stable under faults.

Three elements are considered in this analysis: transient stability, the satisfaction of loads without violation of constraints and voltage stability. These elements will be discussed in the following sections.

Transient stability analysis

The first-swing stability model in a power system is a simple and efficient model to evaluate transient stability [18 - 20]. The power system is considered stable if a fault is cleared before the critical clearing time (CCT). The CCT is defined as the maximum value of fault clearing time (CT). Although a three-phase-fault has a lower probability of occurrence, it has larger impact on a system. Utility companies prepare themselves for the worst case. It is common practice to use three-phase-faults for transient stability studies. The procedure of transient stability study using numerical integration can be summarized as follow:

Step 1: Construct input data including generator and exciter data.

Step 2: Carry out power flow calculations.

Step 3: Calculate initial conditions for dynamic conditions in the pre-fault state and change the admittance matrix including generators.

Step 4: Assume a contingency and solve differential equations by a modified Euler's method.

Step 5: Plot angle curves of generators and decide system stability based on the angle differences.

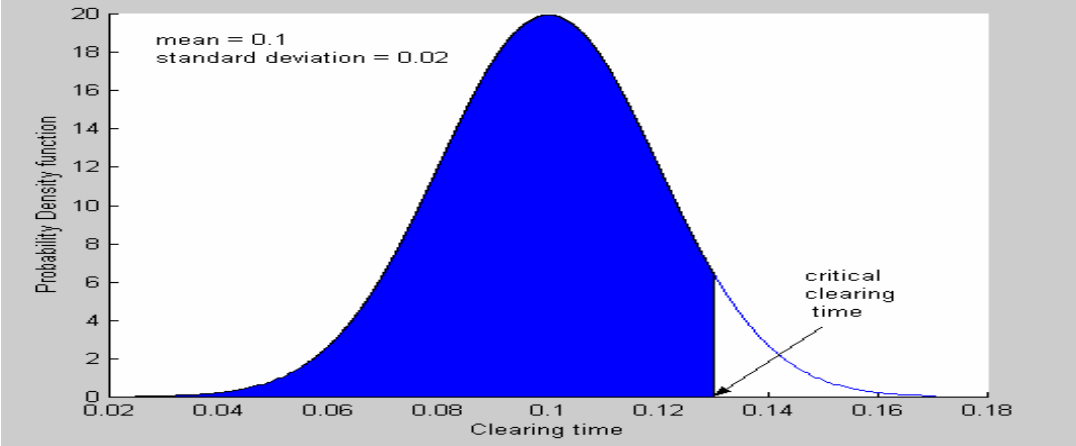

Fig. 2. Probability Density Function for Fault Clearing Time

The evaluation of CCT requires elaborate computations, which include time-consuming solutions of nonlinear system equations. A conventional step-by-step method requires a large amount of computation time for calculating CCT. It is carried out by evaluation of dynamic responses at each step with the increase of CT from zero. To overcome the drawback of a step-by-step method, the bisection method [21, 22] is introduced. First, the probability density function of CT is assumed as a normal distribution with μ_c as its mean value as shown in Fig. 2. As shown in Fig. 3, system stability with a mean value (μ_c) of the limits ($\mu_c \pm 4\sigma_c$) in fault clearing probability density function is decided through steps shown in the procedure of angle stability analysis. When a system is stable, the lower value (CT2) is replaced by mean value of lower and higher value. Otherwise, the mean value of the lower and the higher value replace the higher value (CT1). This procedure is repeated until convergence, which means the difference of the lower value and the higher value is less than 0.01.

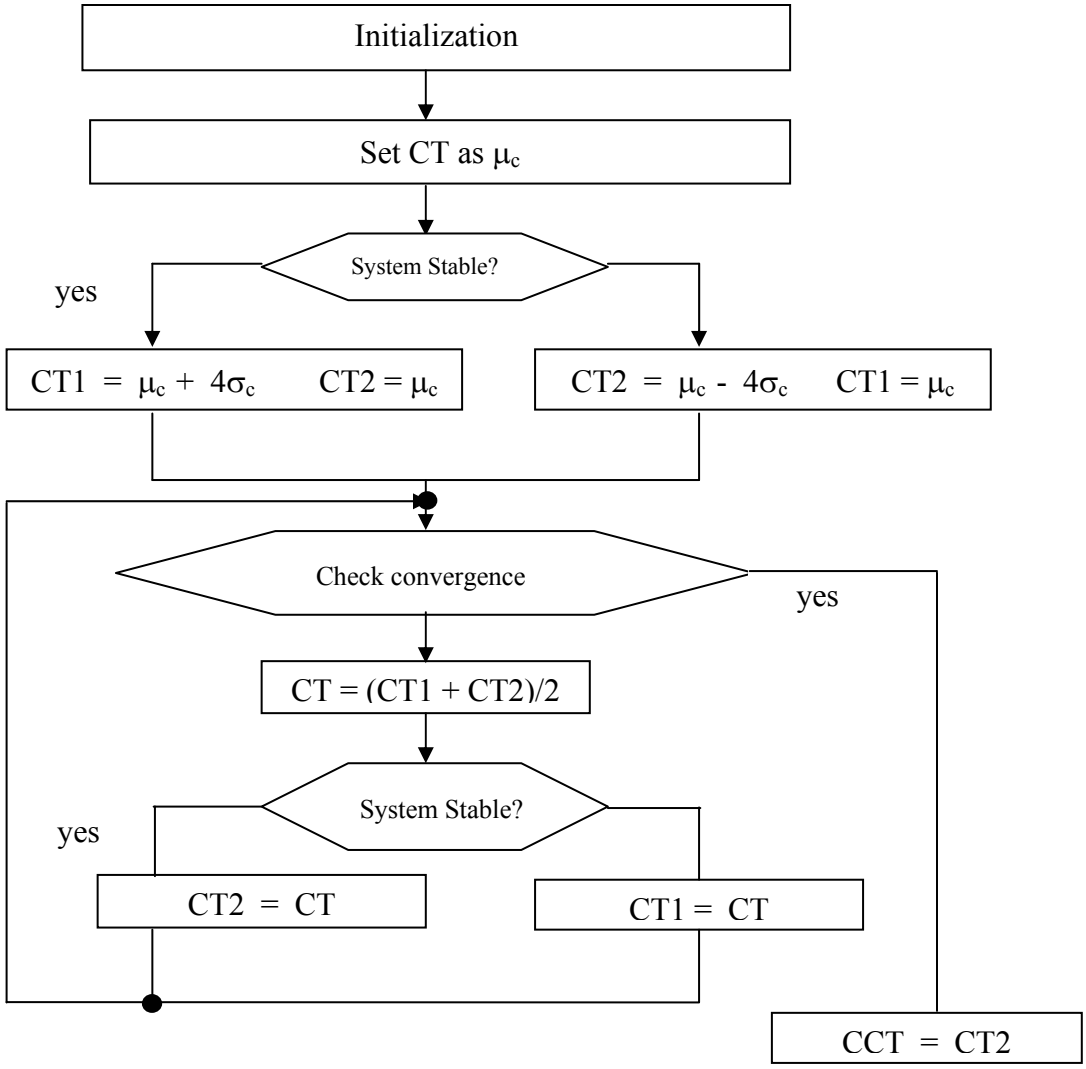

Fig. 3. A Flowchart of CCT Calculation by Bisection Method

We can calculate the probability of successfully clearing a fault ($\mathbf{B_{ts}}$) for the contingency *k* using probability density function of clearing time. That is, for the contingency *k*,

$$B_{ts}(k) = P[CT \le CCT] \tag{3.1}$$

This probability is compared with the minimum acceptable probability of stability (B_{ts}^{min}), which is assumed as 0.6. If B_{ts} is larger than B_{ts}^{min}, B'_{ts} is equal to one. Otherwise, B'_{ts} is equal to zero.

$$B'_{ts}(k) = \begin{cases} 1 & when \quad B_{ts} \geq B_{ts}^{min} \\ 0 & when \quad B_{ts} < B_{ts}^{min} \end{cases} \tag{3.2}$$

Steady state analysis (OPF and voltage stability)

Adequacy studies in power system reliability evaluation relate to load curtailment. Corrective actions in security evaluation are similar to that of adequacy studies. When the generation at some buses cannot be maintained in post contingency, the generation should be rescheduled to avoid the violation of constraints such as the limit of power flows and power generations. To maintain generation-load balance, load shedding may be unavoidable. The optimal power flow (OPF) program is implemented to determine if a system for certain contingency results in the loss of load. The problem is defined as the minimization of active load curtailment in system buses [23]. The quantity of load curtailment (f) is an objective function. When the objective function is not zero, the sampled state may result in the loss of load. For all buses from i=1 to n,

$$\text{Objective function :} \qquad f = \min \sum_{i=1}^{n} X_i \tag{3-3}$$

Subject to:

$$X_i = P_{lireq} - P_{li}$$

$$P_{gi} - P_{li} = \sum_{j=1}^{n} V_i V_j (G_{ij} \cos \delta_{ij} + B_{ij} \sin \delta_{ij})$$

$$Q_{gi} - Q_{li} = \sum_{j=1}^{n} V_i V_j (G_{ij} \sin \delta_{ij} - B_{ij} \cos \delta_{ij})$$

$$P_{gi,min} \leq P_{gi} \leq P_{gi,max}$$

$$Q_{gi,min} \leq Q_{gi} \leq Q_{gi,max}$$

$$PT_{ij}^{2} + QT_{ij}^{2} \leq S_{ij}^{2}$$

$$P_{li} \;/\; P_{lireq} \;=\; Q_{li} \;/\; Q_{lireq}$$

$$0 \;\le\; P_{li} \;\le\; P_{lireq}$$

$$0 \;\le\; Q_{li} \;\le\; Q_{lireq}$$

where

X_i : load curtailment at bus i

P_{lireq}, Q_{lireq} : real and reactive load demands at bus i

P_{li} , Q_{li} : real and reactive power after rescheduling of generation at bus i

P_{gi}, Q_{gi} : real and reactive power generation at bus i

V_i , V_j : voltage magnitude at bus i and j, respectively

$G_{ij} + jB_{ij} = Y_{ij}$: the ij^{th} element in the Y matrix of the power system

δ_{ij} : angle difference between the voltage at bus i

$V_{i,min}$, $V_{i,max}$: minimum and maximum voltage magnitude at bus i, respectively

$P_{gi,min}$, $P_{gi,max}$: minimum and maximum real power generation at generator bus i

$Q_{gi,min}$, $Q_{gi,max}$: minimum and maximum reactive power generation at generator bus i

PT_{ij}, QT_{ij} : real and reactive power flow between bus i and j

S_{ij} : maximum apparent power flow between bus i and j

In the above formulation, the dependent variables are the real and reactive power of a slack bus, reactive power and voltage angle of each *PV* bus, and voltage magnitude and angle of each *PQ* bus. The control variables are load shedding at each load bus, real and reactive power of generator buses, and generator voltage setting. The constraints are briefly described as follows:

- The second and third are real and reactive power balance equations at each system bus.
- The fourth assumes that when the real power of each bus is curtailed, the corresponding reactive power may also be shed to maintain the load power factor constant.

- The rest are inequality constraints, which represent real and reactive power generation limits, thermal-operating limits of transmission lines, the limits of load curtailed at each load bus, and bus voltage limits.

Now, we can express B_{lc} to indicate whether or not load shedding exists for the contingency k. When there is no load shedding for the contingency k, B_{lc} is equal to one. Otherwise, B_{lc} is equal to zero.

$$B_{lc}(k) = \begin{cases} 1 & when \quad f = 0 \\ 0 & when \quad f > 0 \end{cases} \tag{3-4}$$

System instability may also be encountered without loss of synchronism. A system can also become unstable because of voltage collapse caused by a contingency. Voltage stability is considered as a local phenomenon. When a transmission system is represented by a hybrid form as in the equation (3-5), a voltage indicator (L_i) is used in the equation (3-6) to assess the voltage stability of load bus i [11].

$$\begin{bmatrix} V_L \\ I_G \end{bmatrix} = [\ H\ ] \begin{bmatrix} I_L \\ V_G \end{bmatrix} \tag{3-5}$$

where

V_L, V_G : voltage at load or generator bus respectively

I_L, I_G : current at load or generator bus respectively

H : hybrid matrix

The voltage stability indicator [24 -25] shows the portion of the system that is directly affected by a contingency. It varies between zero and one at each load bus. The indicator is zero when there is no load in the system, while it is one at the collapse point. The voltage indicator (L_i) can be expressed in the following equation to assess the voltage stability of load bus i.

$$L_i = \left| \frac{S_{i+}^{*}}{Y_{ii+} \cdot V_i^{2}} \right| \tag{3-6}$$

where

$$S_{i+} = S_i + V_i \sum_{\substack{j \in Load \\ j \neq i}} \frac{Z_{ij}^{*} \cdot S_j}{Z_{ii}^{*} \cdot V_j}$$

$$Y_{ii+} = (Z_{ii})^{-1}$$

S_{i+}^{*} : the conjugate of S_{i+}

S_i : the complex power of bus i

Z_{ij} : the ij^{th} element in the Z matrix of the power system

Z_{ij}^{*} : the conjugate of Z_{ij}

V_i : voltage at bus i

The second term of the complex power (S_{i+}) is expressed as contributions of the other loads to the index at bus i. The voltage stability indicator of the overall system is the maximum value (L_k) among voltage stability indicators of the load buses.

$$L_k = \max(L_i) \tag{3-7}$$

B_{vs} indicates whether voltage at load buses is abnormal or not for the contingency k. This value is compared with the threshold value, which is set as 0.3 for any transmission line fault. When it is less than the threshold value (L_{th}) for the contingency k, B_{vs} is equal to one. Otherwise, B_{vs} is equal to zero.

$$B_{vs}(k) = \begin{cases} 1 & when \quad L_k < L_{th} \\ 0 & when \quad L_k > L_{th} \end{cases} \tag{3-8}$$

Integration of Security-constraints

Transient state and steady state constraints through transient stability, load curtailment, and voltage stability analysis are defined by binary value, zero and one. If a

system violates any of the above conditions for the contingency *k*, the system is in an emergency state. If the system satisfies all of the above conditions for the contingency *k*, the system may be in a normal state or alert state. That is,

$$B_{ss}(k)\begin{cases} = 1 & normal \quad or \quad alert \\ = 0 & emergency \end{cases} \tag{3-9}$$

where $B_{ss}(k) = B'_{ts}(k) \cdot B_{lc}(k) \cdot B_{vs}(k)$

Determination of the indices of normal and alert states based on the system operating state is explained in the next section.

3. Consideration of Additional Contingency

When neither a system problem nor voltage stability problem exists in spite of contingencies, additional contingencies should be considered in order to distinguish the normal state and alert state. The normal state should have a sufficient margin to withstand assumed extra line outages. Additional contingencies, however, should be defined on the basis of probability of system state caused by the absence of the component. Generally, when the probability of line availability for a particular transmission line is one, we do not consider extra line outages for the particular line because it may never fail. Similarly, if the probability of line availability is close to one such as 0.999, assumed extra line outages of that line create some problems. The probabilistic approach can deal with this situation in a better manner.

Under these conditions, additional contingencies should also be considered in order to distinguish between the normal state and alert state. For the contingency *k,* the additional contingency probability in alert state (P_r) is expressed by the equation (3-10).

$$P_r \cong \sum_{\substack{i=1, \\ i \neq k}}^{N} [P_l(i \mid k) \cdot \{1 - B_{ss}(i \mid k)\}] \tag{3-10}$$

where

$P_l(i \mid k)$: Probability of system state for additional contingency i given by the contingency k.

$B_{ss}(i \mid k)$: B_{ss} for additional contingency i given the contingency k.

N : The total number of component

$B_{ss}(i|k)$ is zero if a system for additional contingency i given by the contingency k is in an emergency state, which means that a system for the contingency k is in an alert state. The equation (3-10) basically sums the probability of states where an additional contingency results in emergency states. The additional contingency probability in normal state can be expressed as the complement of the additional contingency probability in alert state. With an N-component system and N' component contingency, $(N\text{-}N')$ calculations are required for state characterization of additional contingencies. For example, $(N\text{-}2)$ calculations are carried out for double contingencies.

C. Probabilistic Security Evaluation by Monte-Carlo Simulation

In complicated systems like power systems, Monte-Carlo simulation is able to model the process with reasonable accuracy. The next event method in sequential Monte-Carlo simulation is used here. The steps for straight Monte-Carlo Simulation including state characterization are as follow:

Step 1: Generate a random number for each component such as a transmission line or a generator and generate its history. The state of the system at any time is defined by the state of its component. This status of states can be represented as a base case, a contingency, double contingencies and so on. The evaluation of double and more contingencies should be handled in security analysis. For example, double contingencies are the overlaps of two outages. They often can make a system insecure, even though a system satisfies operating conditions when either happened separately.

Step 2 : Perform state characterization for each sampled state. When there is a system problem or local problem, which means B_{ss} from the equation (3-8) is zero, update the duration and occurrence number of the emergency state. The index of emergency state is similar to a conventional LOLP (loss of load probability).

Step 3 : Consider additional contingencies when there is neither a system problem nor voltage stability problem to determine whether this is the normal or alert state. Calculation of P_r is described in the previous section. The duration of contingency k, d_s is apportioned into its duration of the alert state as $d_s \cdot P_r$ and its duration of the normal state as $d_s \cdot (1-P_r)$. This information is used in determining D_n^i and D_a^i in equations (3-13) and (3-14). The frequency of contingency k, f_s is apportioned into its frequency of the alert state as $f_s \cdot P_r$ and its frequency of the normal state as $f_s \cdot (1-P_r)$. This information is also used in determining n_n^i and n_a^i in equations (3-13) and (3-14). The expected duration time and the number of occurrences in the normal and alert state per occurrence can be computed as follow:

$$d_n = (1 - P_r) \cdot d_s, \qquad n_n = (1 - P_r) \cdot f_s \tag{3-11}$$

$$d_a = P_r \cdot d_s, \qquad n_a = P_r \cdot f_s \tag{3-12}$$

where

d_s : Duration without a system failure per occurance.

f_s : Occurance without a system failure. Here, f_s is always one.

d_n, n_n : Duration and number of occurances in normal state

d_a, n_a : Duration and number of occurances in alert state

Step 4 : Calculate security indices. The normal, alert and emergency state indices are calculated using equations (3-13), (3-14) and (3-15) respectively. The probability (P_n) and frequency (F_n) of a normal state are

$$P_n = \frac{\sum_{i=1}^{N} (D_n^i)}{N \cdot 8760} \qquad F_n = \frac{\sum_{i=1}^{N} (n_n^i)}{N} \tag{3-13}$$

where

$D_n^i = \sum d_n$: Duration in normal state for *i*th year

$n_n^i = \sum n_n$: Occurence number in normal state for *i*th year

N : Total number of simulation years

The probability (P_a) and frequency (F_a) of an alert state are

$$P_a = \frac{\sum_{i=1}^{N} (D_a^i)}{N \cdot 8760} \qquad F_a = \frac{\sum_{i=1}^{N} (n_a^i)}{N} \tag{3-14}$$

where

$D_a^i = \sum d_a$: Duration in alert state for *i*th year

$n_a^i = \sum n_a$: Occurence number in alert state for *i*th year

The probability and frequency of an emergency state are

$$P_e = 1 - P_n - P_a \qquad F_e = \frac{\sum_{i=1}^{N} (n_e^{'})}{N} \tag{3-15}$$

where

n_e^i : Occurence number in emergency state for *i*th year

Step 5 : Check the coefficient of variation and a maximum iteration number. Repeat above steps until a coefficient of variation is less than a specified threshold or maximum iteration is arrived.

D. Case Studies

1. Application to the WSCC System

One line diagram of the Western System Coordinating Council (WSCC) 3-machine and 9-bus system is shown in Fig. 4. The base MVA is 100 and system frequency is 60 Hz. Detailed data of transmission lines and generators are shown in Table I-(a) and I-(b). Generators and exciters data used in this simulation are given in Table I-(c) and I-(d). The parameters used in tables are described in [26].

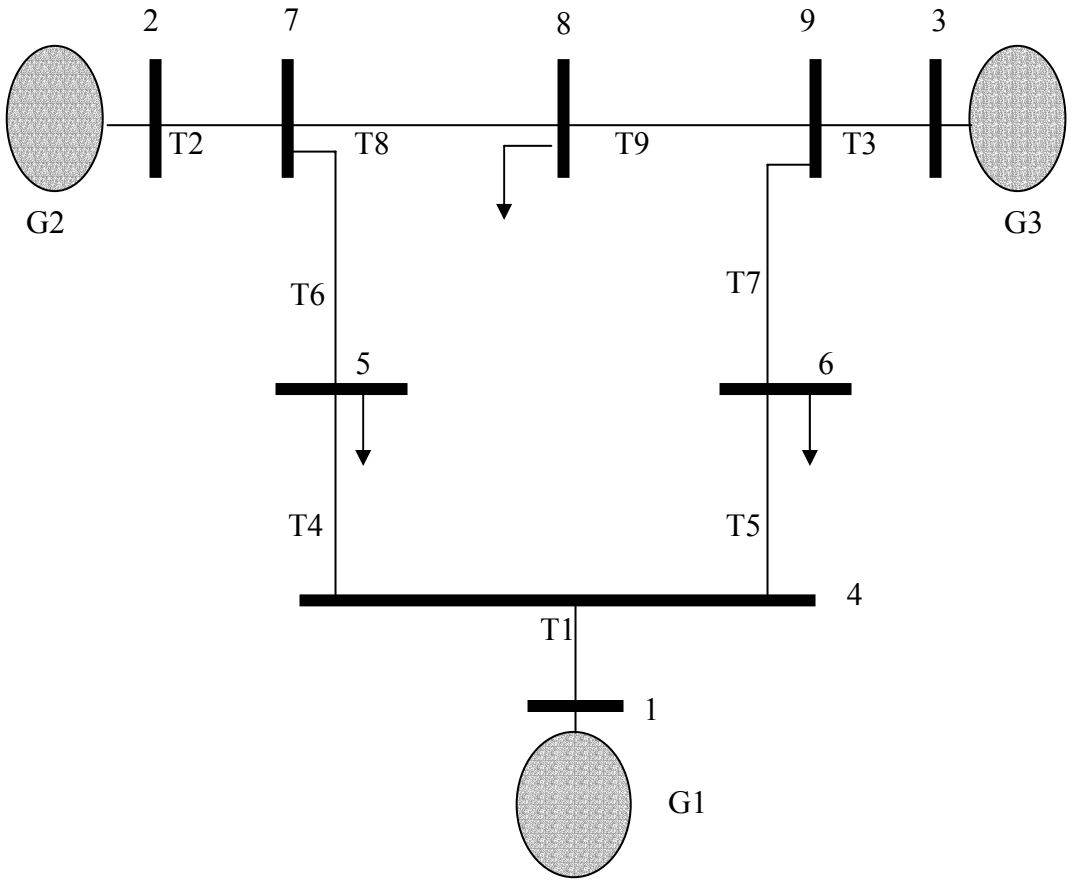

Fig. 4. One Line Diagram of WSCC 9-Bus System

TABLE I. The Data for WSCC System

(a) Branch Data including Fault Clearing Time Probability Distribution Data

Line		R	X	B/2	Limit	Dist.	M.C.T.*	S. D.**
From	To	(p.u.)	(p.u.)	(p.u.)	(MVA)	Type	(sec)	(sec)
1	4	.0000	.0576	.0000	300	Normal	0.20	0.02
2	7	.0000	.0625	.0000	300	Normal	0.20	0.02
3	9	.0000	.0586	.0000	300	Normal	0.20	0.02
4	5	.0100	.0850	.0880	300	Normal	0.20	0.02
4	6	.0170	.0920	.0790	300	Normal	0.20	0.02
5	7	.0320	.1610	.1530	300	Normal	0.05	0.02
6	9	.0390	.1700	.1790	300	Normal	0.10	0.02
7	8	.0085	.0720	.0745	300	Normal	0.10	0.02
8	9	.0119	.1008	.1045	300	Normal	0.15	0.02

* Mean clearing time

** Standard Deviation

(b) Bus Data

Bus No.	Pg (MW)	Qg (MVAR)	Pd (MW)	Qd (MVAR)	|V|	Angle
1	71.6	27	0.0	0.0	1.040	0
2	163.0	6.7	0.0	0.0	1.025	9.3
3	85.0	-10.9	0.0	0.0	1.025	4.7
4	0.0	0.0	0.0	0.0	1.026	-2.2
5	0.0	0.0	125.0	50.0	0.996	-4.0
6	0.0	0.0	90.0	30.0	1.013	-3.7
7	0.0	0.0	0.0	0.0	1.026	3.7
8	0.0	0.0	100.0	35.0	1.016	0.7
9	0.0	0.0	0.0	0.0	1.032	2.0

TABLE I. (continued)

(c) Generator Data

Generator No.	H(s)	Xd	Xd'	Xq	Xq'	Td0'	Tq0'
1	23.6400	0.1460	0.0608	0.0969	0.0969	8.9600	0.3100
2	6.4000	0.8958	0.1198	0.8645	0.1969	6.0000	0.5350
3	3.0100	1.3125	0.1813	1.2578	0.2500	5.8900	0.6000

(d) Exciter Data

Generator No.	KA	KE	KF	TA	TE	TF	KSe	Tse
1	20.0	1.000	0.063	0.200	0.314	0.350	0.0039	1.555
2	20.0	1.000	0.063	0.200	0.314	0.350	0.0039	1.555
3	20.0	1.000	0.063	0.200	0.314	0.350	0.0039	1.555

State Characterization

For simplification, failure rates and repair rates of all generators are assumed as λ_G = *1.5e-3 [1/hours]* and μ_G = *0.1 [1/hours]* respectively. Failure rates and repair rates of all transmission lines are also assumed as λ_T = *1.5e-5 [1/hours]* and μ_T = *0.1 [1/hours]* respectively. All possible contingency cases are considered, which includes independent overlapping contingencies.

To determine transient stability, the angle difference of generators is investigated. An example of angle curves, when clearing time is 0.83 with a fault on line 5-7, is shown in Fig. 5. The angle curve of all generators is similar, and the system is stable. The determination of critical clearing time is performed by the bisection method as explained the previous section. The result of critical clearing time by the bisection method and the probability of successfully clearing fault (B_{ts}) for each line contingency is shown in Table II-(a).

Table II-(b) shows the voltage stability indicator of the overall system and different load buses for a contingency of each line. In case of the contingency in line 8-9, voltage stability indicator of load bus 8 has the largest value.

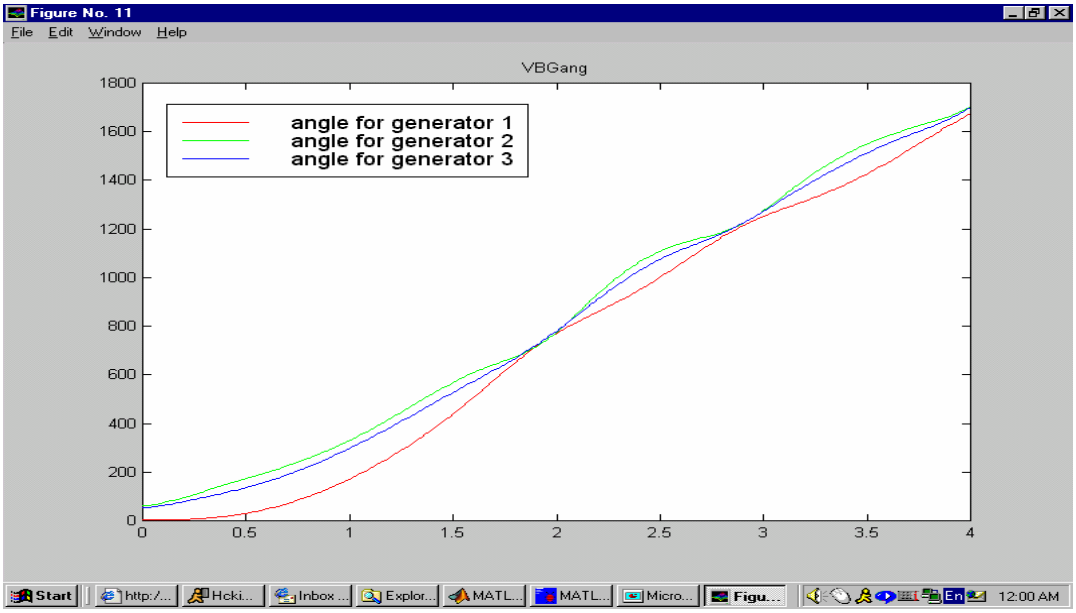

Fig. 5. The Angle Curves of Each Generator
(when clearing time is 0.83 and fault is Line 5-7 in WSCC System)

Table II. An Example of State Characterization

(a) The Result of Critical Clearing Time and the Probability of Transient Stability

Line		Critical clearing time (sec)	Probability of transient stability
From	To		
1	4	0.12	0.0000
2	7	0.12	0.0000
3	9	0.12	0.0000
4	5	0.23	0.9332
4	6	0.24	0.9772
5	7	0.08	0.9332
6	9	0.13	0.9332
7	8	0.165	0.9994
8	9	0.185	0.9599

Table II (continued)

(b) The Voltage Stability Indicator of the Overall System and Different Load Buses by the Location of Contingency

Line		Voltage stability indicator						
From	To	Bus No.						Overall system
		4	5	6	7	8	9	
1	4	0.4079	**0.4311**	0.3835	0.1306	0.1744	0.1118	0.4311
2	7	0.1134	**0.2433**	0.1709	0.2310	0.2253	0.0950	0.2433
3	9	0.1075	0.1911	**0.2027**	0.1039	0.1918	0.1958	0.2027
4	5	0.0398	**0.5023**	0.1068	0.1284	0.1501	0.0623	0.5023
4	6	0.0551	0.1418	**0.2972**	0.0706	0.1243	0.0849	0.2972
5	7	0.1124	**0.2563**	0.1596	0.0433	0.0954	0.0549	0.2563
6	9	0.1053	0.1819	**0.2092**	0.0680	0.1017	0.0364	0.2092
7	8	0.0828	0.1564	0.1474	0.0410	**0.2108**	0.0861	0.2108
8	9	0.0818	0.1716	0.1253	0.0971	**0.1840**	0.0307	0.1840

(c) The Result of Transient State (B_{ts}), Load Curtailment (B_{lc}), and Voltage Stability (B_{vs}), and Combined Result B_{ss} for Each Line Outage

Outage No.	Line		B_{ts}	B_{lc}	B_{vs}	B_{ss}
	From	To				
T1	1	4	0	0	0	0
T2	2	7	0	0	1	0
T3	3	9	0	0	1	0
T4	4	5	1	1	0	0
T5	4	6	1	1	1	1
T6	5	7	1	1	1	1
T7	6	9	1	1	1	1
T8	7	8	1	1	1	1
T9	8	9	1	1	1	1

The voltage stability index of the overall system is the largest (0.1840) among voltage stability indicators for each bus. This value is compared with a threshold value. When it is larger than the threshold value, the system is near to a collapse point. Here, the threshold point is set as 0.3. Because voltage stability indicators of the line 1-4 and line 4-5 are larger than the threshold point, the overall system is regarded as unstable in the contingency of the line 1-4 and 4-5.

Together with OPF and voltage stability analysis in steady state, the integrated security for each line contingency is shown in Table II-(c). Transmission line contingencies 1-4, 2-7, 3-9, and 4-5 relate to the emergency state.

Analytical Method

Analytical methods can obtain accurate results if all the states in the state spaces can be enumerated. For an N component system with k-order contingency, the number of simulations is ${}_NC_k$. When considering a system with 1000 components, this would be 499,500 for double contingencies and 166,167,000 for triple contingencies and so on.

Table III lists the results of transient stability, load curtailment and voltage stability for various contingencies. There are twelve system elements with three generators and nine transmission lines. The total number of contingencies including the base case is ${}_{12}C_1 + {}_{12}C_2 + \text{-------} + {}_{12}C_{11} + {}_{12}C_{12}$. With contingencies higher than single order, the system appears always insecure in this case.

The probability for an emergency state can be easily obtained by the enumeration approach. The probability for a normal and an alert state can be obtained after computing the additional contingency probability in alert state. The frequency of each state can be obtained by equivalent transition rate [3]. The probability and frequency for each state using analytical methods is shown in Table IV.

Table III. The Combined Result B_{ss} for Each Contingency Case

No	Contingency	B_{ss}	No	Contingency	B_{ss}	No	Contingency	B_{ss}
1	No outage	1	28	G2,T6	0	55	T2,6	0
2	G1	0	29	G2,T7	0	56	T2,7	0
3	G2	0	30	G2,T8	0	57	T2,8	0
4	G3	0	31	G2,T9	0	58	T2,9	0
5	T1	0	32	G3,T1	0	59	T3,4	0
6	T2	0	33	G3,T2	0	60	T3,5	0
7	T3	0	34	G3,T3	0	61	T3,6	0
8	T4	0	35	G3,T4	0	62	T3,7	0
9	T5	1	36	G3,T5	0	63	T3,8	0
10	T6	1	37	G3,T6	0	64	T3,9	0
11	T7	1	38	G3,T7	0	65	T4,5	0
12	T8	1	39	G3,T8	0	66	T4,6	0
13	T9	1	40	G3,T9	0	67	T4,7	0
14	G1,T1	0	41	G1,2	0	68	T4,8	0
15	G1,T2	0	42	G1,3	0	69	T4,9	0
16	G1,T3	0	43	G2,3	0	70	T5,6	0
17	G1,T4	0	44	T1,2	0	71	T5,7	0
18	G1,T5	0	45	T1,3	0	72	T5,8	0
19	G1,T6	0	46	T1,4	0	73	T5,9	0
20	G1,T7	0	47	T1,5	0	74	T6,7	0
21	G1,T8	0	48	T1,6	0	75	T6,8	0
22	G1,T9	0	49	T1,7	0	76	T6,9	0
23	G2,T1	0	50	T1,8	0	77	T7,8	0
24	G2,T2	0	51	T1,9	0	78	T7,9	0
25	G2,T3	0	52	T2,3	0	79	T8,9	0
26	G2,T4	0	53	T2,4	0	80	G1,2,3	0
27	G2,T5	0	54	T2,5	0	81	More than 3rd	0

Table IV. Probabilities and Frequencies by Analytical Method for WSCC System

	Analytical method	
	Probability (%)	Frequency (occ./year)
Emergency State	0.0443	38.178
Alert State	0.0416	1.6616
Normal State	0.9141	36.493

Monte-Carlo Simulation

The simulation is repeated until it reaches a specified number of years or convergence is less than a specified convergence criterion. In this simulation, the maximum number of simulation years is set as 300 and the coefficient of variation is set as 0.5 for convergence criterion. The probability and frequency for each state using Monte-Carlo Simulation is shown in Table V. When comparing with analytical methods, the probability and frequency for each state are almost the same.

Table V. Probabilities and Frequencies by MCS for WSCC System

	Monte-Carlo Simulation	
	Probability (%)	Frequency (occ./year)
Emergency State	0.0431	39.8800
Alert State	0.0417	1.7201
Normal State	0.9152	37.7699

2. Application to the IEEE RTS

The IEEE Reliability Test System (RTS) is a 24-bus system with 38 transmission lines. The annual system peak load is 2850 [MW]. The total installed generating capacity is 3405 [MW]. The one line diagram of the system is shown in Fig. 6. IEEE RTS is described in detail in [27]. The exciter is assumed to be identical for all machines and is of the IEEE Type I. The machine is represented by a two-axis model. Probability distribution data of fault clearing time, generator and exciters data are shown in Table VI.

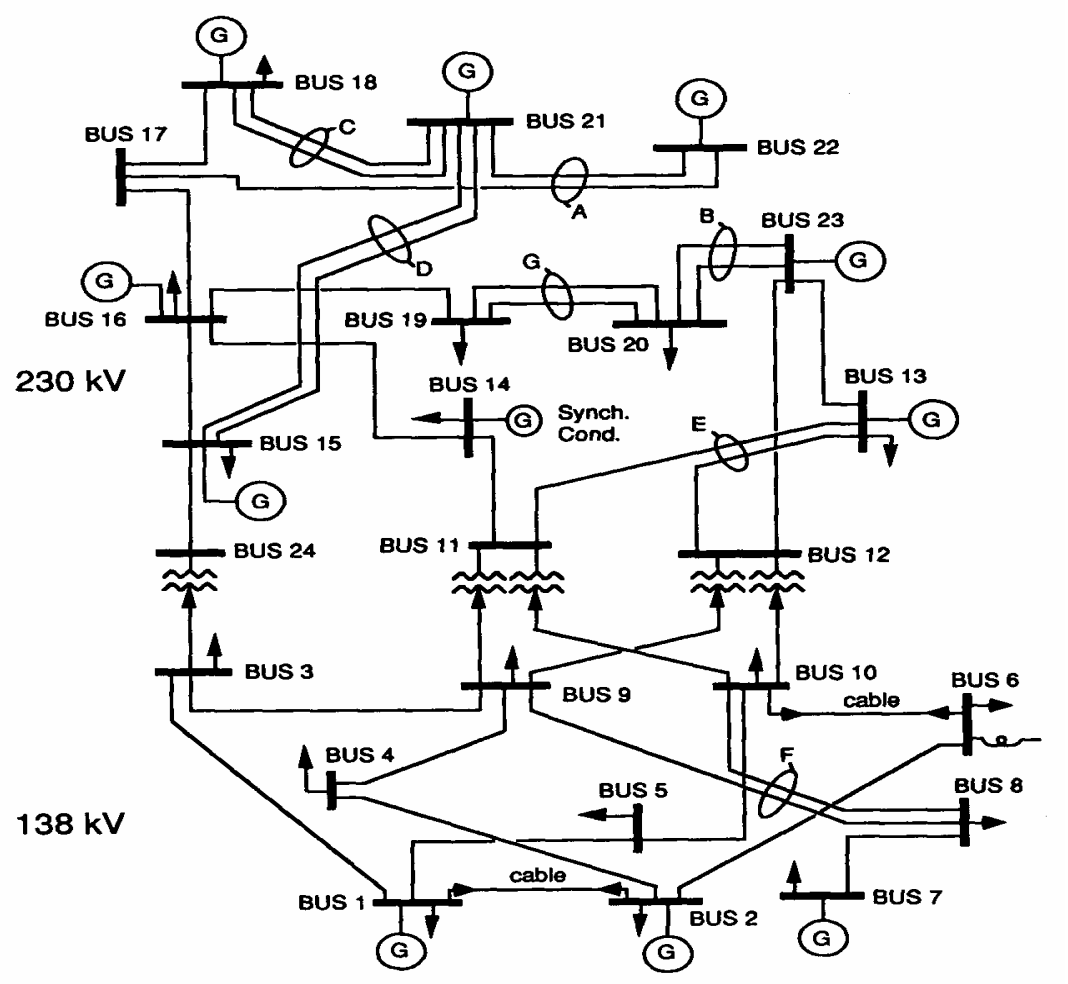

Fig. 6. One Line Diagram of IEEE Reliability Test System

TABLE VI. The Data for IEEE RTS
(a) Fault Clearing Time Probability Distribution Data

Line		Type of Distribution	Mean clearing time (sec)	Standard Deviation (sec)
From	To			
1	2	Normal	0.15	0.02
1	3	Normal	0.05	0.02
1	5	Normal	0.20	0.02
2	4	Normal	0.20	0.02
2	6	Normal	0.20	0.02
3	9	Normal	0.08	0.02
3	24	Normal	0.08	0.02
4	9	Normal	0.20	0.02
5	10	Normal	0.20	0.02
6	10	Normal	0.15	0.02
7	8	Normal	0.15	0.02
8	9	Normal	0.20	0.02
8	10	Normal	0.20	0.02
9	11	Normal	0.15	0.02
9	12	Normal	0.15	0.02
10	11	Normal	0.15	0.02
10	12	Normal	0.15	0.02
11	13	Normal	0.15	0.02
11	14	Normal	0.15	0.02
12	13	Normal	0.20	0.02
12	23	Normal	0.20	0.02
13	23	Normal	0.20	0.02
14	16	Normal	0.15	0.02
15	16	Normal	0.15	0.02
15	21	Normal	0.15	0.02
15	21	Normal	0.15	0.02
15	24	Normal	0.15	0.02
16	17	Normal	0.15	0.02
16	19	Normal	0.15	0.02
17	18	Normal	0.15	0.02
17	22	Normal	0.20	0.02
18	21	Normal	0.15	0.02
18	21	Normal	0.15	0.02
19	20	Normal	0.15	0.02
19	20	Normal	0.15	0.02
20	23	Normal	0.15	0.02
20	23	Normal	0.15	0.02
21	22	Normal	0.20	0.02

TABLE VI. (continued)

(b) Generator Data

Gen. No.	H(s)	Xd	Xd'	Xq	Xq'	Td0'	Tq0'
1	23.6400	0.1460	0.0608	0.0969	0.0969	8.9600	0.3100
2	6.4000	0.8958	0.1198	0.8645	0.1969	6.0000	0.5350
7	3.0100	1.3125	0.1813	1.2578	0.2500	5.8900	0.6000
13	23.6400	0.1460	0.0608	0.0969	0.0969	8.9600	0.3100
14	6.4000	0.8958	0.1198	0.8645	0.1969	6.0000	0.5350
15	3.0100	1.3125	0.1813	1.2578	0.2500	5.8900	0.6000
16	23.6400	0.1460	0.0608	0.0969	0.0969	8.9600	0.3100
18	6.4000	0.8958	0.1198	0.8645	0.1969	6.0000	0.5350
21	3.0100	1.3125	0.1813	1.2578	0.2500	5.8900	0.6000
22	6.4000	0.8958	0.1198	0.8645	0.1969	6.0000	0.5350
23	23.6400	0.1460	0.0608	0.0969	0.0969	8.9600	0.3100

(c) Exciter Data

Gen. No.	KA	KE	KF	TA	TE	TF	KSe	Tse
1	20.0	1.000	0.063	0.200	0.314	0.350	0.0039	1.555
2	20.0	1.000	0.063	0.200	0.314	0.350	0.0039	1.555
7	20.0	1.000	0.063	0.200	0.314	0.350	0.0039	1.555
13	20.0	1.000	0.063	0.200	0.314	0.350	0.0039	1.555
14	20.0	1.000	0.063	0.200	0.314	0.350	0.0039	1.555
15	20.0	1.000	0.063	0.200	0.314	0.350	0.0039	1.555
16	20.0	1.000	0.063	0.200	0.314	0.350	0.0039	1.555
18	20.0	1.000	0.063	0.200	0.314	0.350	0.0039	1.555
21	20.0	1.000	0.063	0.200	0.314	0.350	0.0039	1.555
22	20.0	1.000	0.063	0.200	0.314	0.350	0.0039	1.555
23	20.0	1.000	0.063	0.200	0.314	0.350	0.0039	1.555

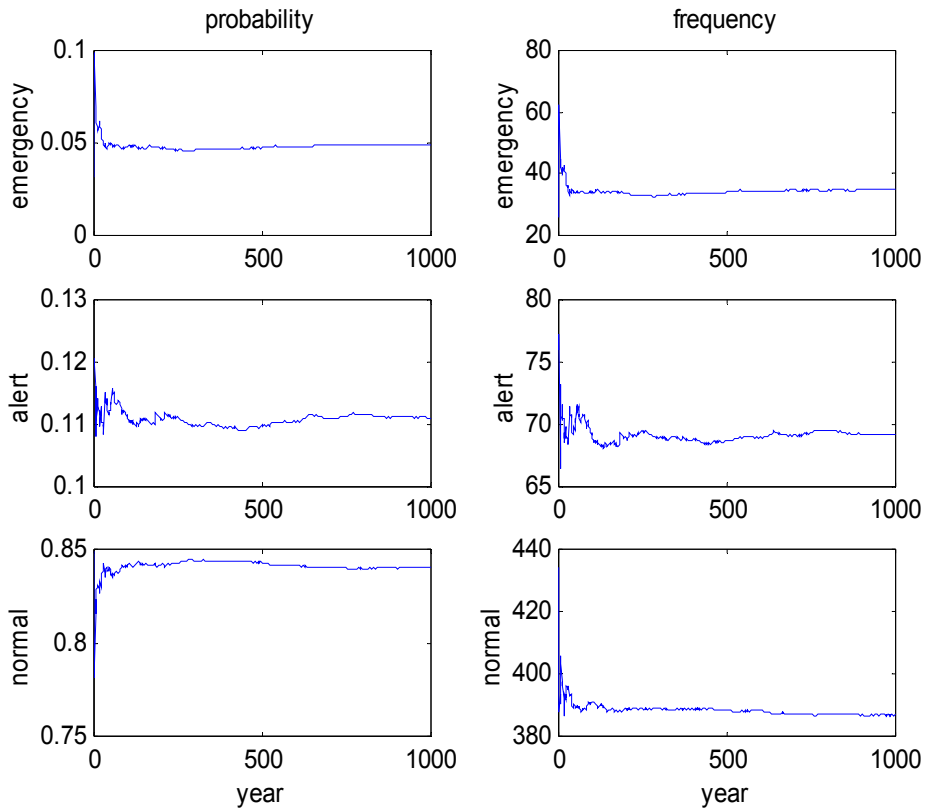

Fig. 7. The Plot of Probabilities and Frequencies for Each State with 95% Load

One example of Monte-Carlo simulation is shown in Fig. 7. The plot of probabilities and frequencies is converging with repeated simulations. The simulation can be continued until a specified maximum year. The percentage of the load means the percentage of each maximum load for each load bus. The 100 % load is the annual system peak load, which is the sum of maximum loads of each bus. The simulation results with 100%, 95%, 90%, and 75% load are shown in Table VII. As system load is decreased, the system becomes more secure. The probability for the normal state is slightly increased as a load level percentage decreases.

TABLE VII. Probabilities and Frequencies of MCS for IEEE RTS

Load	Probability (%)			Frequency (occ./year)		
	Normal	Alert	Emergency	Normal	Alert	Emergency
100%	0.6921	0.2053	0.1026	309.61	109.09	72.04
95%	0.8442	0.1107	0.0450	389.12	68.80	32.83
90%	0.9174	0.0619	0.0208	428.92	45.69	23.46
75%	0.9712	0.0255	0.0033	463.86	23.46	3.48

E. Summary

A probabilistic method for security assessment is proposed in this Chapter. State characterization is carried out by transient stability analysis for dynamic effects and by voltage stability analysis and OPF for static effects. The application to the WSCC system shows the accuracy of Monte-Carlo simulation compared with the analytical method for security assessment. The analytical method, when evaluating the frequency and duration indices, is relatively complex and the actual system needs to be simplified for mathematical modeling. Due to these disadvantages of the analytical method, Monte-Carlo simulation is one of the most widely used in power system reliability evaluations. The application to IEEE RTS indicates that Monte-Carlo simulation for security assessment can be extended to the analysis of more complicated systems.

CHAPTER IV

PROBABILISTIC SECURITY ANALYSYS USING KOHONEN NETWORKS AND MONTE-CARLO SIMULATION

A. Problem Formulation

Artificial neural network is one of the emerging and exciting developments in solving engineering problems such as computer vision, control and speech recognition. They mimic the human biological neural nets, which can learn how to recognize and classify pattern in an autonomous manner. In power systems, artificial neural networks have also been used in many areas, e.g. load forecasting, security assessment, fault diagnosis, system identification, and voltage control [28 - 34].

The cerebral cortex in human physiology is the center for diverse activities such as thinking, speech, vision and hearing. The specific regions of the cortex have their own role and are located consistently relative to one another. These regions can be referred to as ordered feature maps. For example, there exists the tonotopic map of auditory regions where neighboring neurons respond to similar sounds. This clustering mechanism of human brain led researchers to the concept of Kohonen Networks. Kohonen networks, which were developed by Teuvo Kohonen during the early 1980s, can be used in classification problems [35 - 36]. Kohonen networks are divided into two main subgroups based on the learning philosophy: supervised and unsupervised learning. Supervised learning needs the correct desired output for a controlled adaptation to minimize the error between the neural output and the desired output. Learning Vector Quantization (LVQ) is a pattern classification method in the supervised learning class. The combination of Learning Vector Quantization and Monte-Carlo simulation is called the LVQ-MCS in this Chapter. In unsupervised learning, the learning process classifies similar data into clusters using similarity indices. Self-organizing maps (SOM) learn to recognize groups of similar input vectors in such a manner that neurons physically near each other in the neuron layer respond to similar input vectors. The combination of Self-organizing maps and Monte-Carlo simulation is called the SOM-MCS in this

dissertation. The main purpose of LVQ-MCS is to avoid time-consuming characterization of sampled state in Monte-Carlo simulation. SOM-MCS overcomes the computation burden caused by repeated characterization of similar states. Therefore, the comparison of two different approaches would provide useful information in the power system reliability evaluation.

For many applications, the Kohonen networks can perform more accurate classification than Backpropagation networks. The approaches using Backpropagation networks may be extremely time-consuming and need a huge amount of learning data [30]. This is why Kohonen networks are proposed in combination with Monte-Carlo simulation for security assessment in power systems.

This Chapter proposes a new probabilistic method involving transient stability and voltage stability for power system security assessment by combining Monte-Carlo simulation and Kohonen Networks. The main disadvantage of the use of straight Monte-Carlo simulation for reliability and security analysis is the time required for the characterization of sampled states. The proposed approach overcomes the problem of a large amount of computation time required of straight Monte-Carlo simulation. Data classification by Kohonen networks can reduce sampling data. This reduces computation time for reliability security indices when using classified data. The case study of IEEE RTS is presented to demonstrate the efficiency of both SOM-MCS and LVQ-MCS approaches.

The framework would be useful for operational and long term planning. In operational planning, an indication of the degree of security breach provides important information to operators. For example, if the probability of alert or emergency state is too high, the generation may not cover the system load in near future. To avoid load shedding, system operators may decide additional generating units to be started. In long-term planning, the degree of security breach gives information to system planners for generation or transmission expansion schemes.

B. Self-Organizing Map (SOM)

1. Structure of Self-Organizing Map

The structure of SOM is shown in Fig. 8. SOM consists of a standard input layer and a Kohonen layer. Each input neuron is connected to every neuron in the Kohonen layer. This Kohonen layer learns to categorize its input vectors. After computing the distance between input vectors and weight vectors, Kohonen layer identifies a winner neuron through competitive transfer functions. All neurons that lie within a neighborhood surrounding the winning neuron are allowed to adjust their weights. Neurons that are outside the neighborhood do not adjust their weights. All neurons within a certain neighborhood of the winning neuron are updated using the Kohonen-rule. Kohonen-rule is explained in the algorithm in the next section.

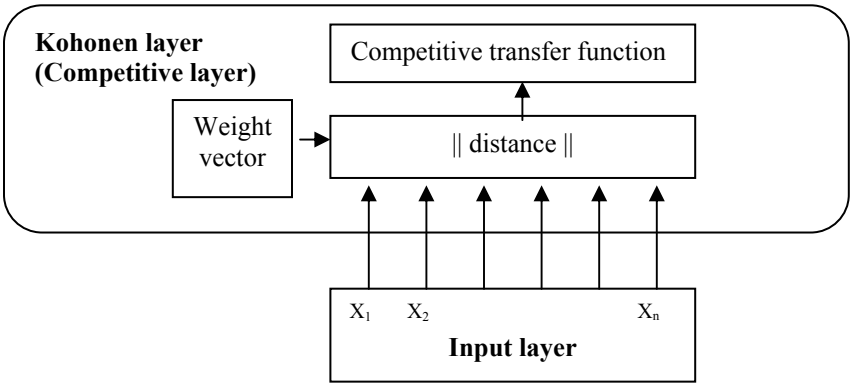

Fig. 8. Structure of Self-Organizing Maps

2. Algorithm of Self-Organizing Map

Each neuron *j* in the Kohonen layer is represented by an *(n+m)* dimensional weight vector w_j = [w_{j1} w_{j2} ---$w_{j(n+m)}$]. The input vectors to the SOM are represented by X = [X_1 X_2 --- X_i --- X_o] where *o* is the number of the input vectors. The dimension of each input vector is the same as that of the weight vector. The input vector in our studies is the selected contingencies described in the next section. The dimension of weight vector is the same as the sum of the number of transmission lines (*n*) and the number of

generation buses (*m*). The algorithm to map the system states into the neuron is described below.

Step 1 : Initialize weight vectors and decide the parameters of SOM such as topology, distance function and learning rate.

Step 2 : Start learning while a stopping condition is satisfied (Repeat step 3-10). Here, a stopping condition is indicated by $w_j(t+1) \approx w_j(t)$.

Step 3 : For each input vector X_i, repeat steps 4-6.

Step 4 : Compute Euclidean distances between neurons and a input vector X_i.

$$d_j = \sqrt{\sum_{i=1}^{n} (X_i - w_j(t))^2} \tag{4-1}$$

where

X_i : the *i* th input vector.

$w_j(t)$: the *j* th weight vector at time t.

Step 5 : Find a winner neuron *j* with the minimum distance.

$$c = \arg\min d_j \tag{4-2}$$

Step 6 : Update weight vectors ($w_j(t)$) within a specified neighborhood for a winner neuron using Kohonen -rule.

$$w_j(t+1) = w_j(t) + a(t) \cdot h_{cj}(t) \cdot (X_i(t) - w_j(t)) \quad \text{for } j \in h_{cj}(t) \tag{4-3}$$

$$w_j(t+1) = w_j(t) \quad \text{for } j \notin h_{cj}(t) \tag{4-4}$$

where

$a(t)$: learning rate

$h_{cj}(t)$: topological neighborhood

Step 7 : Update learning rate ($a(t)$), which is a monotonically decreasing function.

Step 8 : Reduce the radius of topological neighborhood ($h_{cj}(t)$).

Step 9 : Increase the iteration number $t = t+1$.

Step 10 : Check stopping condition.

The basic idea of SOM is the vicinity concept based on the distance between neurons and each input vector, which means input data near a neuron may match this neuron. Only a neuron with a minimum distance between input vectors and a weight vector is updated in the equation (4-3) or (4-4) until the current weight vector is the same as the previous. The state of neuron called by weight vectors changes its value during learning. The final weight vectors, called the state of neurons, are only taken as input data for the state characterization.

The selection of topology including the number of map units (the number of neurons), the lattice type and the map dimension is one of the most important factors to obtain satisfactory results. The number of map units and map dimension may increase as the number of input vectors increases. There are three different topologies for the original neuron locations such as grid, hexagonal, rectangular, and random topology.

The learning structure has important parameters such as the map initialization, the neighborhood function and the learning rate function. There are three kinds of map initialization; random, linear or hexagonal. If random initialization is chosen, a different result may be obtained. The neighborhood function has several possible choices such as bubble, Gaussian, cut Gaussian, and Ep function. The learning rate starts at the ordering-phase (Rough-tuning) and decreases until it reaches the tuning-phase (Fine-tuning). The learning rate continues to decrease very slowly during the tuning-phase. The neighborhood size shrinks and learning rate value within the neighborhood also decreases towards zero. Both the shrinkage of neighborhood and the decrease in the learning rate change slowly.

The optimal selection of topology and learning structure is based on the quantization error. The quantization error is defined as the mean of $\| x - w_c \|$ over all learning states where x is the input learning vector and w_c is the nearest weight vector to x.

C. Learning Vector Quantization (LVQ)

1. Structure of Learning Vector Quantization

While SOM categorizes similar input vectors without the use of learning data to specify a typical member of each group, learning in LVQ is accomplished by presenting a sequence of patterns with an associated target output vector.

LVQ classifies input data into groups that it determines. The network can be trained to classify inputs while preserving the inherent topology of the learning set, i.e., nearest neighbor relationships in the learning set are preserved while input patterns that have not been previously learned are categorized into their nearest neighbors. The structure of LVQ is essentially the same as SOM without a second linear layer for target class as shown in Fig. 9. The linear layer transforms the competitive layer's classes into target classifications defined by users.

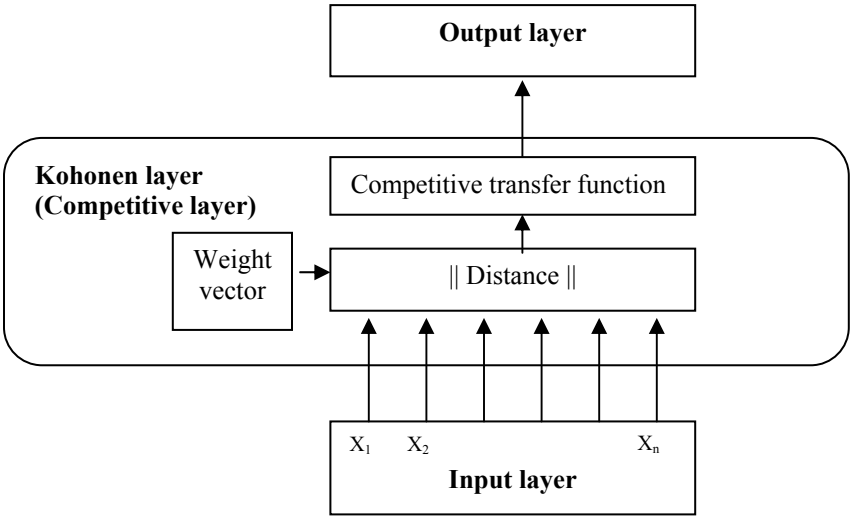

Fig. 9. Structure of Learning Vector Quantization.

The features of LVQ are as follows: 1) LVQ is a supervised learning neural network, which has teacher's signal as a target class. 2) While weight vector in SOM is updated within a specified neighborhood, only the weight vector which is closest to

input vectors is updated in LVQ. 3) No neighborhood around a winner is defined during learning in LVQ.

2. Algorithm of Learning Vector Quantization

Each neuron j of the Kohonen layer in LVQ is represented by an $(n+m+1)$ dimensional weight vector $w_j = [\ w_{j1}\ w_{j2}\ \text{---}w_{j(n+m)}\ o_j\ ]$ including the output o_j. The input vector to the SOM is represented by $X = [\ X_1\ X_2\ \text{---}\ X_i\ \text{---}\ X_p\ ]$ where p is the number of the input vectors. The dimension of each input vector is the same as that of the weight vector. The basic steps of the algorithm are listed as follows:

Step 1 : Initialize weight vectors and decide the parameter of LVQ such as topology, distance function and learning rate.

Step 2 : Start learning while a stopping condition is satisfied (Repeat step 3-9). Here, a stopping condition is indicated by $w_j(t+1) \approx w_j(t)$.

Step 3 : For each input vector X_i, repeat steps 4-6.

Step 4 : Compute Euclidean distances between neurons and input vector X_i as shown in the equation (4-1).

Step 5 : Find a winner neuron j with minimum distance as shown in the equation (4-2).

Step 6 : Update weight vector ($w_j(t)$) as follows:

When $T = C_j$

$$w_j(t+1) = w_j(t) + a(t) * (x_i(t) - w_j(t)) \tag{4-5}$$

When $T \neq C_j$

$$w_j(t+1) = w_j(t) - a(t) * (x_i(t) - w_j(t)) \tag{4-6}$$

where T : A target class for learning vector

C_j : class represented by j *th* output unit

Step 7 : Update a learning rate ($a(t)$), which is monotonically a decreasing function.

Step 8 : Increase the iteration number $t = t+1$.

Step 9 : Check a stopping condition.

D. Kohonen Networks Application for Security Analysis

1. Implementation of Kohonen Networks

The dimension and elements of input vector

A power system state consists of the status of transmission lines and generators. The input vector corresponding to a system state can be represented as:

SOM : $X_i = [\, T_1\ T_2$ ----- T_l -----$T_n\ G_1\ G_2$ ----- G_k ----- $G_m\,]$

LVQ : $X_i = [\, T_1\ T_2$ ----- T_l -----$T_n\ G_1\ G_2$ ----- G_k ----- $G_m\ \ C_i\,]$

where

T_l : The status of transmission line l.

(T_l =1 : k th transmission line is up state,

T_l =0 : k th transmission line is down state)

G_k : Normalized available real power generation of bus k.

(When several units are connected at one bus, G_k is the sum of all the available real power of each unit)

C_i : Target class for i th input data.

n : The total number of transmission lines.

m : The total number of generation buses.

The dimension of an input vector is an important factor for learning the SOM or LVQ. As the dimension of input vectors increases, more learning time is needed because the structure becomes more complicated. For example, if the status of each generator unit occupies an element of the input vector and several units are connected at one bus, the dimension of input vector may be increased and corresponding input format may cause difficulty of learning.

There are two kinds of input elements for SOM: the status of transmission lines and magnitude of available generations. While the former is only represented as zero (down state) and one (up state), the latter is a normalized value between zero and one (maximum real power generation) because several units are connected at one bus.

Normalization of input vector elements is important so that none of them have a disproportionate influence on learning. The transformation for normalization ensures that input vector elements from zero to very large numbers are within the range from zero to one: x'= (available real power generation) / (maximum capacity).

The dimension and input vector elements of LVQ are the same as those of SOM except a target class (C_i), which results from the state characterization by OPF and stability calculations. If a system satisfies operating conditions after the state characterization, a target class is represented as "one".

State characterization

As discussed in the Chapter III, three elements for state characterization are considered in these analyses: transient stability, satisfaction of load without violation of constraints and voltage stability.

The selection of learning sets

The selection of learning sets for both SOM and LVQ is also an important factor for getting desirable results. Learning sets of SOM can be easily obtained by the random sampling as those of Monte-Carlo simulation. The reason is that these learning sets do not all need to use OPF and stability analysis. For optimal learning, it is desirable to include all types of contingency data in learning sets. In order to reflect all kinds of contingencies, the contingency type with low occurrence probability should be emphasized for learning set of SOM. Otherwise, the contingency type with high occurrence probability has an overwhelming influence on learning. The suitable combination of two contingency types plays a key role for getting desirable results.

On the other hand, all learning sets of LVQ cannot be obtained by the random sampling like those of SOM. If all learning sets of LVQ are obtained by the random sampling, each sample from random sampling needs the state characterization to get a target class. This means that we can't reduce computation time because of a large number of state characterizations. LVQ learning sets also consist of two kinds: the

contingency types with high occurrence probabilities and the contingency type with low occurrence probabilities. Some contingency types (e.g. one generating unit contingency) occur frequently. These types in LVQ should be selected not by random sampling but by all possible contingency situations. Since the others seldom occur, it's more convenient to select these by random sampling than considering all situations. The selection of all possible situations in the contingency types with high occurrence probabilities avoids repeated sample data. The selection by random sampling in the contingency types with low occurrence probabilities reflects all kinds of contingency types for desirable learning. Both learning sets contribute to the reduction of input data.

Flowchart of Kohonen networks

Flowcharts for Kohonen network implementation in power system security analysis are shown in Fig. 10. In case of SOM, input vectors of component states match the weighting vectors of neurons after the learning process. The state corresponding to weighting vectors of neurons only is taken as component states for the OPF and stability calculations. These calculations are made on the states of mapped neurons. The mapped neuron is labeled as secure or insecure after OPF and stability calculations. These calculations are made on the states of mapped neurons. The mapped neuron is labeled as "one" or "zero" after state characterization.

For LVQ, the state characterization for each contingency decides the class (target vector) before the learning process. The class of output vectors is divided into two classes, "one" and "zero". Note that we don't need to do OPF and stability analysis repeatedly for each contingency. After making input vector and target vector, we need to create LVQ. We can train LVQ to perform a particular function by adjusting the values of the connections between elements. In general, neural networks are trained so that a particular input leads to a specific target output. The neural network is adjusted, based on a comparison of the output and the target, until the network output matches the target.

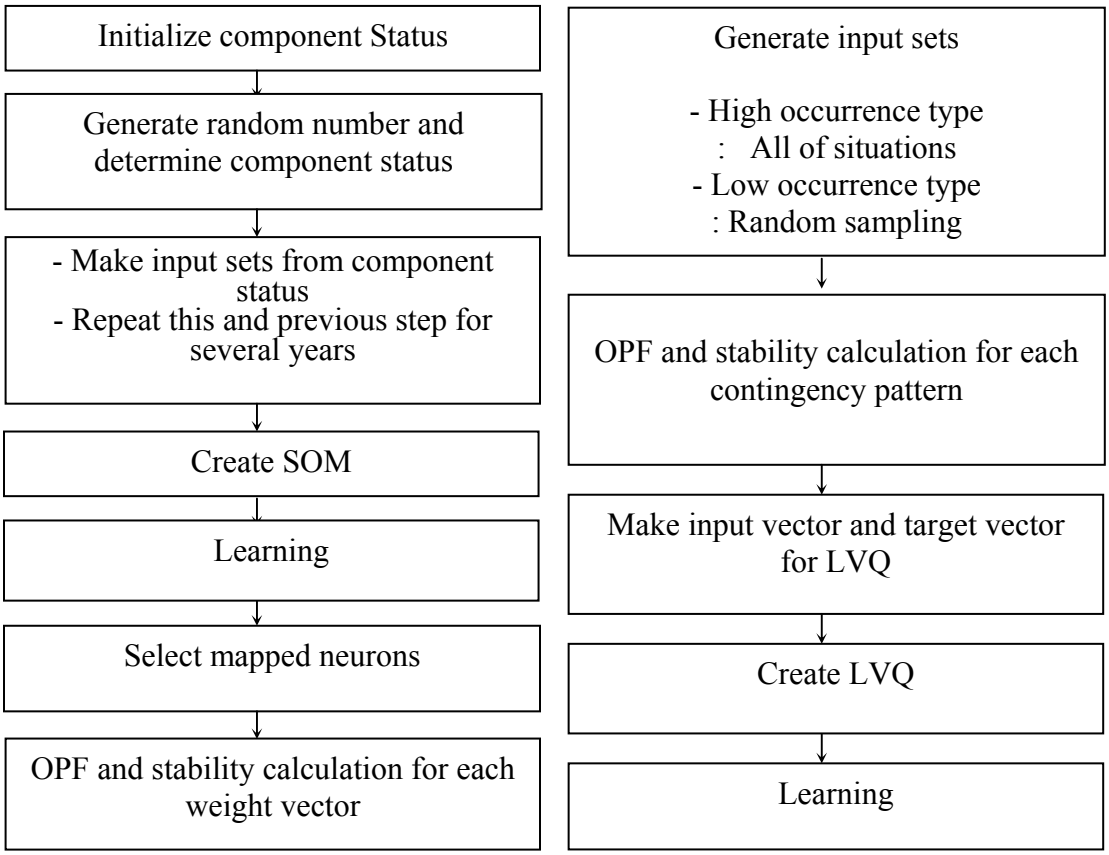

a) SOM b) LVQ

Fig. 10. Flowcharts of Kohonen Networks Application for Security Assessment

2. Security Assessment Using SOM-MCS and LVQ-MCS

A flowchart of SOM-MCS or LVQ-MCS for security assessment is shown in Fig. 11. The procedure is the same as straight Monte-Carlo Simulation except the state characterization, the evaluation of security breach for sampled states. While straight Monte-Carlo Simulation requires the procedure of state characterization during simulation, SOM-MCS and LVQ-MCS can obtain the result of state characterization by on-line use.

Like Monte-Carlo simulation, SOM-MCS or LVQ-MCS can use random sampling for contingencies. Input learning patterns are generated from the history of the system generated by using random numbers and failure rate and repair rate of components. The target class of a sampled state, even if not used in learning data, can be checked through the on-line use of trained SOM or LVQ. The target class of states in expected additional contingencies is also carried out not by OPF and stability analysis but by on-line use of SOM or LVQ.

When there is neither a system problem nor voltage stability problem, additional contingencies determine whether this is normal or alert state. After computing additional contingency probability, the duration of contingency k is apportioned into its duration of alert state and its duration of normal state. The frequency of contingency k is also apportioned into its frequency of alert state and its frequency of normal state. The security index, the probability and frequency of normal, alert, and emergency, is calculated as the same way in Chapter III.

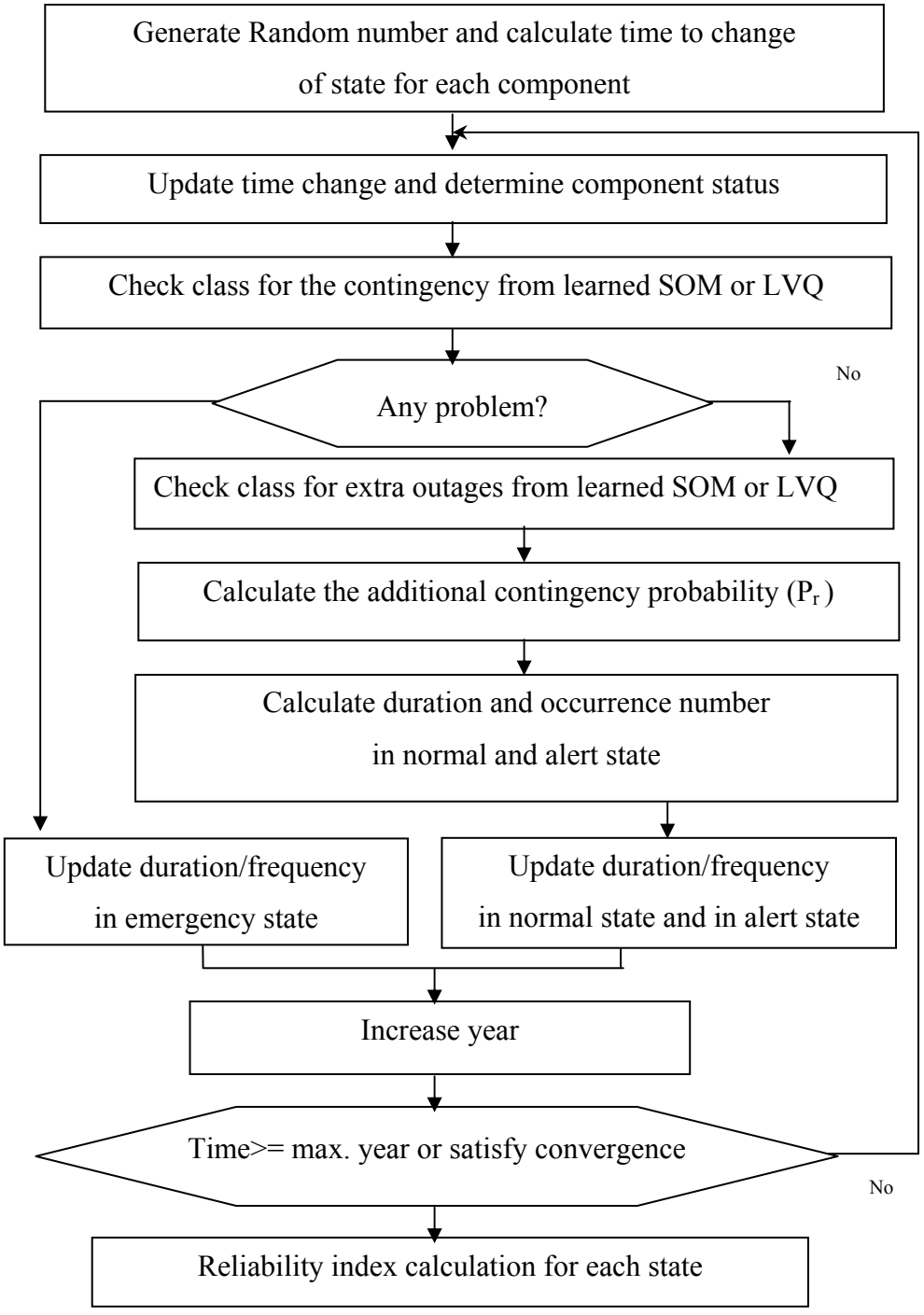

Fig. 11. A Flowchart of SOM-MCS or LVQ-MCS

3. Computation Time Efficiency

The objective of the proposed method is to reduce the large amount of computation time required by the straight Monte-Carlo simulation. In General, the computation time of Monte-Carlo simulation depends on the number of OPF and stability calculation. Total simulation time(T_m) is

$$T_m \cong J_m \cdot T1 + \alpha 1 \tag{4-7}$$

where

$T1$: The average state characterization time per event.

$\alpha 1$: The other Monte-Carlo simulation time

$J_m \cong (\text{events / per year}) \cdot (\text{h years}) \cdot (1 + p \cdot N)$

J_m : The number of OPF and stability calculation in Monte-Carlo simulation

N : The average of the number of additional outage, which depend on the number of transmission lines and generator units

p : The probability of normal and alert state

h : Simulation years

On the other hand, the number of state characterization in SOM-MCS is the number of mapped weight vectors (J_s), which depends on the number of SOM input vectors. The number of mapped weight vectors is less than the number of weight vectors. Total simulation time (T_{sm}) can be expressed as

$$T_{sm} \cong J_s \cdot T1 + T_s + \alpha 2 \tag{4-8}$$

where

T_s : Learning time for SOM.

$\alpha 2$: The processing time for SOM-MCS in Fig. 11.

The time of T_s is very small when compared with J_s*$T1$. The processing time α is the same as that of Monte-Carlo simulation. Since the number of the state

characterizations in straight Monte-Carlo simulation is much more than the number of mapped weight vectors, the burden of computation is reduced.

Suppose that the number of the state characterizations for LVQ-MCS is J_L. While the simulation time of SOM-MCS depends on the number of mapped weight vectors, LVQ-MCS depends directly on the number of input vectors. The smaller the number of input vectors is, the more the computation time may be reduced. Total simulation time (T_{LM}) is

$$T_{LM} \cong J_L \cdot T1 + T_L + \alpha 3 \tag{4-9}$$

where

T_L : Learning time for LVQ.

$\alpha 3$: The processing time for LVQ-MCS in Fig. 11.

Similar to SOM-MCS, T_L is also very small when compared with J_L*$T1$. In general, learning time of LVQ is longer than that of SOM. Only characterization of input vectors may make the computation simpler compared with straight Monte-Carlo simulation. Meanwhile, LVQ-MCS simulation time is more than SOM-MCS simulation time. The reason is that only the mapped neurons need to use state characterization in SOM-MCS.

It's difficult to exactly guess the simulation time of large or real systems due to the complexity of systems, the transition rates, simulation years and the selection of optimal neural network. Compared with the straight Monte-Carlo simulation, the computation times of SOM-MCS and LVQ-MCS, however, increase to a lesser degree. The use of SOM-MCS and LVQ-MCS is suitable for analysis of a complicated system.

E. Case Studies : IEEE Reliability Test System

The IEEE RTS, a 24-bus system with 38 transmission lines, is described in Chapter III. We used SOM_PAK program for simulation, which is demonstrated in *SOM Toolbox 2.0* [35].

1. Case I : When Considering Only Transmission Line Faults

Tables VIII shows the characteristics of the SOM and LVQ with only transmission line contingencies. The dimension of input data in both SOM and LVQ is thirty-eight because IEEE RTS has thirty-eight transmission lines. To obtain optimal SOM, all of parameters such as lattice type, initialization, neighborhood and learning rate function are tested based on quantization error. Here, the minimum of quantization error in SOM is 0.009 when SOM includes rectangular for the lattice type, linear function for map initialization, Ep function for the neighborhood type.

TABLE VIII. The SOM and LVQ Characteristics for Case I

(a) Self-Organizing Maps

Input data	Dimension	38
	The number of learning patterns	1038
Topology	The number of map units	154
	Lattice type	Rectangular
Learning structure	Map initialization	Linear
	Neighborhood type	Ep
	Learning rate function	Linear
	Ordering-phase initial learning rate	0.5
	Tuning-phase initial learning rate	0.05

TABLE VIII. (continued)

(b) Learning Vector Quantization

Input layer	Dimension	38
	The number of Learning patterns	634
Topology	The number of map units	156
	Lattice type	Rectangular
Learning structure	Map initialization	Linear
	Learning rate	0.05

Since the structure of LVQ is almost the same as that of SOM, the parameters of LVQ are selected based on SOM. Due to computation burden, SOM is carried out with fixed learning rates, e.g. 0.5 for ordering-phase initial learning rate and 0.05 for tuning-phase initial learning rate respectively. The change of learning rate may cause better SOM for classification. The number of neurons in a competitive layer is decided as 154 for SOM and 156 for LVQ respectively. In general, the number of map units depends on the number of learning sets.

The probability and frequency for each state by SOM-MCS and LVQ-MCS with only transmission line contingencies is shown in Table IX. Five simulations at each load level are also shown. Maximum simulation year is set as 100 but with different seeds. The percentage of load represents total system load level. For example, 100% load is the sum of maximum loads of each bus and 90% load means the sum of 90% of maximum loads of each bus. With smaller load, the probability and frequency of normal state increase smoothly and the system can be operated more safely.

TABLE IX. Probabilities and Frequencies for Case I

(a) SOM-MCS by Load Change

Load		Probability (%)			Frequency (occ./year)		
		Normal	Alert	Emer.	Normal	Alert	Emer.
100 %	Case1	.9862	.0070	.0068	22.89273	0.162279	5.414994
	Case2	.9856	.0070	.0073	22.76461	0.162279	5.543109
	Case3	.9858	.0070	.0072	22.23792	0.159432	6.075498
	Case4	.9857	.0070	.0072	22.53685	0.159432	5.773716
	Case5	.9860	.0070	.0070	22.62796	0.162279	5.679765
95 %	Case1	.9912	.0046	.0043	25.02513	0.116727	3.33099
	Case2	.9915	.0046	.0039	25.04221	0.116727	3.311061
	Case3	.9902	.0046	.0052	24.55253	0.11388	3.803592
	Case4	.9905	.0046	.0049	24.78598	0.11388	3.570138
	Case5	.9909	.0046	.0045	25.07353	0.116727	3.279744
90 %	Case1	.9928	.0036	.0036	25.79667	0.093951	2.582229
	Case2	.9945	.0036	.0039	25.79382	0.093951	2.585076
	Case3	.9928	.0036	.0036	25.9561	0.093951	2.41995
	Case4	.9936	.0036	.0029	25.85076	0.093951	2.525289
	Case5	.9925	.0036	.0039	25.96749	0.093951	2.408562
75 %	Case1	.9947	.0027	.0026	26.70771	0.074022	1.688271
	Case2	.9946	.0027	.0027	26.61091	0.074022	1.785069
	Case3	.9942	.0027	.0031	26.59952	0.074022	1.796457
	Case4	.9943	.0027	.0029	26.51696	0.074022	1.87902
	Case5	.9949	.0027	.0023	26.77604	0.074022	1.619943

TABLE IX. (continued)

(b) LVQ-MCS by Load Change

Load		Probability (%)			Frequency (occ./year)		
		Normal	Alert	Emer.	Normal	Alert	Emer.
100 %	Case1	.9824	.0088	.0088	22.73614	0.202137	5.531721
	Case2	.9840	.0088	.0072	22.48561	0.19929	5.785104
	Case3	.9833	.0088	.0079	22.60233	0.202137	5.668377
	Case4	.9820	.0088	.0092	22.26069	0.19929	6.012864
	Case5	.9832	.0088	.0081	22.50269	0.19929	5.765175
95 %	Case1	.9886	.0063	.0051	24.93403	0.159432	3.376542
	Case2	.9878	.0063	.0059	24.79737	0.159432	3.516045
	Case3	.9898	.0063	.0039	24.96534	0.159432	3.345225
	Case4	.9877	.0063	.0060	24.79168	0.159432	3.521739
	Case5	.9892	.0063	.0045	25.03937	0.159432	3.271203
90 %	Case1	.9902	.0053	.0045	25.71695	0.139503	2.613546
	Case2	.9895	.0053	.0052	25.75396	0.139503	2.576535
	Case3	.9917	.0053	.0030	25.77959	0.139503	2.550912
	Case4	.9911	.0053	.0036	25.91909	0.139503	2.414256
	Case5	.9892	.0053	.0054	25.74542	0.139503	2.587923
75 %	Case1	.9951	.0027	.0022	26.75041	0.074022	1.645566
	Case2	.9947	.0027	.0026	26.71055	0.074022	1.685424
	Case3	.9946	.0027	.0027	26.74187	0.074022	1.654107
	Case4	.9942	.0027	.0030	26.58529	0.074022	1.810692
	Case5	.9943	.0027	.0029	26.53119	0.074022	1.864785

Table X shows the difference of probability and frequency of SOM-MCS and LVQ-MCS compared with that of straight Monte-Carlo simulation respectively. The probability and frequency of SOM-MCS and LVQ-MCS can be obtained by the average

values among five cases. We can see that SOM-MCS and LVQ-MCS can classify the contingencies with reasonable accuracy.

TABLE X. The Accuracy of Proposed Methods for Case I

(a) The Difference between SOM-MCS and Straight Monte-Carlo simulation

Load	Probability Difference			Frequency Difference		
	Normal	Alert	Emer.	Normal	Alert	Emer.
100%	0.0023	0.0018	0.0005	0.273312	0.039858	0.233454
95%	0.0026	0.0017	0.0012	0.461214	0.042705	0.424203
90%	0.0029	0.0017	0.0009	0.375804	0.042705	0.333099
75%	0.0003	0.0000	0.0003	0.293241	0	0.293241

(b) The Difference between LVQ–MCS and Straight Monte-Carlo simulation

Load	Probability Difference			Frequency Difference		
	Normal	Alert	Emer.	Normal	Alert	Emer.
100%	0.0005	0.0000	0.0005	0.179361	0	0.179361
95%	0.0007	0.0000	0.0007	0.472602	0.002847	0.478296
90%	0.0002	0.0000	0.0003	0.287547	0.002847	0.290394
75%	0.0004	0.0000	0.0003	0.310323	0	0.318864

(c) The Probabilities and Frequencies of Straight Monte-Carlo simulation

Load	Probability (%)			Frequency (occ./year)		
	Normal	Alert	Emer.	Normal	Alert	Emer.
100%	0.9835	0.0088	0.0077	22.33756	0.19929	5.933148
95%	0.9879	0.0063	0.0058	24.43295	0.156585	3.883308
90%	0.9901	0.0053	0.0046	25.49489	0.136656	2.838459
75%	0.9942	0.0027	0.0030	26.34899	0.074022	2.04984

Table XI compares the computation time for the various approaches. It can be seen that SOM–MCS and LVQ-MCS have much less computation time than conventional MCS due to reduced time for OPF and Stability calculations. Since only mapped neurons in SOM-MCS require state characterization, SOM-MCS has less computation burden than LVQ-MCS. Here, the maximum year of Monte-Carlo simulation is 100 years. The classification accuracy is 99.81 % for SOM–MCS and 99.94% for LVQ-MCS.

TABLE XI. The Comparison of Computation Time for Case I

	SOM-MCS	LVQ-MCS	Straight MCS
Computation time (sec)	5124.6	8321.5	913,432.0

2. Case II : When Considering Transmission Line and Generating Unit Faults

Table XII shows the characteristics of the SOM and LVQ with transmission line, generating unit, and both of elements contingencies. The dimension of input data for both SOM and LVQ is forty-eight because IEEE RTS has thirty-eight transmission lines and ten generator buses.

TABLE XII. The SOM and LVQ Characteristics for Case II

(a) Self-Organizing Maps

Input data	Dimension	48
	The number of learning patterns	2394
Topology	The number of map units	238
	Lattice type	Rectangular
Learning structure	Map initialization	Linear
	Neighborhood type	Ep
	Learning rate function	Linear
	Ordering-phase initial learning rate.	0.5
	Tuning-phase initial learning rate.	0.05

TABLE XII. (continued)

(b) Learning Vector Quantization with 100% Load

Input layer	Dimension	48
	The number of Learning patterns	3964
Topology	The number of map units	238
	Lattice type	Rectangular
Learning structure	Map initialization	Linear
	Learning rate	0.05

(c) Learning Vector Quantization with 95% Load

Input layer	Dimension	48
	The number of Learning patterns	2701
Topology	The number of map units	238
	Lattice type	Rectangular
Learning structure	Map initialization	Linear
	Learning rate	0.05

(d) Learning Vector Quantization with 90% Load

Input Layer	Dimension	48
	The number of Learning patterns	2279
Topology	The number of map units	234
	Lattice type	Rectangular
Learning structure	Map initialization	Linear
	Learning rate	0.05

TABLE XII. (continued)

(e) Learning Vector Quantization with 75% Load

Input layer	Dimension	48
	The number of Learning patterns	1472
Topology	The number of map units	234
	Lattice type	Rectangular
Learning structure	Map initialization	Linear
	Learning rate	0.05

As shown in Table XII, the parameters of SOM are always constant in spite of load change if optimal SOM is selected. The reason is that state characterization of mapped neurons is required after recognizing groups of similar input vectors. Since there is an output for each input vector, LVQ needs new parameters in order to get optimal results when different loads are applied.

When discussing the number of learning patterns, the classification of contingencies provides useful information for choosing learning sets as shown in Table XIII. For optimal learning, it is desirable to include all types of data in learning sets and to select as few input vectors as possible. The learning pattern in SOM consists of random sampling for one year for all contingencies and for 30 years for selected contingencies (type 1, 3,4,7,8,9,10 and 11), which results in the quantity of learning patterns. Unfortunately, there is no rule how many years of data should contribute to optimal learning. In case of IEEE RTS, based on experience, 30 years may be recommended for desirable results. The learning patterns in LVQ may be different as load changes. For example, with 95% load, it consists of all possible data of type 0, 2 and 5 and selected data with “class zero” target from random sampling for 50 years (type 1, 3,4, 6, 7, 8, 9, 10 and 11).

TABLE XIII. The Contingency Type for Case II

Type	Description	Probability (%)
0	Base case	12.05
1	one transmission line contingency	1.01
2	one generating unit contingency	29.03
3	One transmission line + one generating unit contingency	1.94
4	Two transmission lines contingency	0.02
5	two generating units contingency	28.42
6	Three generating units contingency	16.16
7	four generating units contingency	2.33
8	One transmission line + two generating units contingency	1.57
9	One transmission lines + one or more generating units contingency	1.12
10	two transmission lines + one or more generating units contingency	0.08
11	The others	6.28

The probability and frequency of SOM-MCS and LVQ-MCS for each state for different load level is shown in Table XIV. Each simulation is carried out for 300 years or until convergence is satisfied. This result can be a little different when using different seeds. As system load is decreased, a system becomes more secure. The probability of normal state increases a little as percentage load level decreases.

Table XV shows the difference of probabilities and frequencies comparing proposed methods and straight Monte-Carlo simulation. The probabilities and frequencies of only MCS are shown in Chapter III. SOM-MCS or LVQ-MCS can approximately classify the power system states for security assessment in the power system. Classification accuracy of SOM-MCS is similar to that of LVQ-MCS.

TABLE XIV. Probabilities and Frequencies for Case II

(a) SOM- MCS

Load	Probability (%)			Frequency (occ./year)		
	Normal	Alert	Emer.	Normal	Alert	Emer.
100%	.7051	.1794	.1155	318.74	95.16	76.85
95%	.8060	.1211	.0730	377.29	65.12	48.34
90%	.9207	.0504	.0289	444.08	27.48	19.19
75%	.9947	.0028	.0025	486.97	1.37	2.40

(b) LVQ-MCS

Load	Probability (%)			Frequency (occ./year)		
	Normal	Alert	Emer.	Normal	Alert	Emer.
100%	.7353	.1722	.0924	327.18	100.99	62.57
95%	.8476	.1017	.0508	398.05	57.57	35.19
90%	.9325	.0445	.0230	445.45	27.29	18.01
75%	.9898	.0067	.0035	483.73	3.83	3.19

TABLE XV. The Accuracy of Proposed Methods for Case II

(a) The Difference between SOM-MCS and Straight Monte-Carlo Simulation

Load	Probability Difference			Frequency Difference		
	Normal	Alert	Emer.	Normal	Alert	Emer.
100%	.0130	.0253	.0129	9.128	13.937	4.809
95%	.0382	.0104	.0280	11.827	3.681	15.508
90%	.0033	.0115	.0081	15.164	18.207	4.270
75%	.0235	.0227	.0008	23.409	22.084	1.080

TABLE XV. (continued)

(b) The Difference between LVQ-MCS and Straight Monte-Carlo Simulation

Load	Probability Difference			Frequency Difference		
	Normal	Alert	Emer.	Normal	Alert	Emer.
100%	.0432	.0331	.0102	17.569	8.097	9.472
95%	.0034	.0090	.0058	8.932	11.238	2.356
90%	.0151	.0174	.0022	16.538	18.403	5.447
75%	.0186	.0188	.0002	19.875	19.630	0.294

From the Table XVI, it can be seen that SOM-MCS and LVQ-MCS have much less computation time than straight Monte-Carlo simulation due to the reduced time for state characterization. Since only mapped neurons in SOM-MCS require state characterization, SOM-MCS has less computation burden than LVQ-MCS. In straight Monte-Carlo simulation, the repeated state characterization of base case is excluded in order to reduce computation burden.

TABLE XVI. The Comparison of Computation Time for Case II

	SOM-MCS	LVQ-MCS	straight MCS
Computation time (min)	1142.56	3821.38	113,245.12

F. Summary

This Chapter has proposed a probabilistic method for security assessment employing SOM-MCS or LVQ-MCS. An example considered in the study (IEEE RTS) shows that the Kohonen networks can not only approximately classify power system states, but also contributes to reduction in total computation time due to decreased number of states to be characterized. In security analysis, state characterization including transient stability, voltage stability and load curtailment for each sampling state is a difficult and time-consuming work. This effort is reduced by the employment of SOM-MCS or LVQ-MCS. Even though SOM-MCS has less computation time than LVQ-MCS, the accuracy of classification of stochastic samples by LVQ is similar to that of SOM. The construction of LVQ-MCS including the selection of learning vector is more difficult than that of SOM-MCS and it needs a different structure according to the change of loads.

It should be remarked that although the neural network based methods do have a small probability of misclassification, this is not as critical for the purpose of computation of probabilistic indices as for some other applications. The computation of indices requires an accumulation of results of classification of many cases. The misclassification of a very small percentage of contingencies may cause some approximation in the index but this is not much different than many other sources of approximation in computing probabilistic indices.

It is also encouraging to see that neural networks for security assessment purposes are being attempted to real power systems. Reference [37] shows a 783-bus system in actual use at Hydro-Québec's operations planning department is tested for contingency screening. Due to a larger number of transmission lines and generators, power systems are more complicated in the actual industrial settings. It is thus important to extract the key elements so as to reduce the dimension of the input vector. Determination of these discriminatory feature vectors could require some further study.

CHAPTER V

SECURITY ANALYSIS FOR SYSTEM OPERATION USING BAYES CLASSIFIER

A. Problem Formulation

In power system operation, on-line security assessment is one of the important issues. Faster methods are required for on-line security assessment since the system may be operating closer to security boundaries with smaller safety margins in the deregulated environment.

When a contingency causes violation of operating limits (e.g. line capacity or voltage limits), the system is insecure or unsafe. One of the conventional methods in security assessment is using a deterministic criterion in which certain contingency cases such as sudden removal of a power generator or loss of a transmission line are studied. Such an approach is computationally time consuming for operating decisions due to a large number of contingency cases to be studied. Moreover, when local phenomenon such as voltage stability is considered for contingency analysis, computation burden is even more increased. For on-line use, excessive computation time in security assessment still remains an unsolved problem.

In order to alleviate these drawbacks, power system security assessment can be treated as a pattern classification problem. A number of approaches using artificial neural networks (ANN) such as back-propagation and Self Organizing Maps [28-34] have been applied for security assessment in power systems over the past decade. The practical implementation of these methods for security assessment, however, has not been fully accomplished in the industry. The key problem of ANN is the determination of optimal ANN architecture, which is decided by trial and error in the selection of number of neurons in the hidden layer. The Bayes classifier can overcome the drawbacks of ANN. Although the Bayes classifier has been applied to various areas such as signal processing, it has seldom been used in power system applications. Recently a few papers based on the Bayesian rule [38-41] have been published in the field of power system applications. The reference [38] suggests a Bayesian-based classification method for forecasting power

market clearing prices. The reference [39] presents a method based on Bayesian estimation for identification of parallel flows.

This Chapter shows how a Bayes classifier [42 - 43] can be implemented for security assessment. As applied to pattern classification, the fundamental role of a Bayes classifier is similar to that of ANN. After the selection and analysis process of feature vectors, system security can be tested by the Bayes decision rule. The security status in a Bayes classifier is decided on the basis of maximum value of Bayes decision function, while that of ANN is determined by interpolating new data with a known security status.

B. Bayes Classifier and Decision Rule

Consider one of the n classes to which a feature vector x may belong. The joint probability density of a feature vector x and a class i can be expressed as follow.

$$p(x,c_i) = p(x|c_i) \cdot P(c_i) \tag{5-1}$$

where

$p(x|c_i)$: the conditional probability density function for the feature vector x, given that it belongs to class c_i.

$P(c_i) = 1/n$: the prior probability of class c_i.

When assuming equal prior probabilities for every class, the assignment of the feature vector to the class with the highest prior probability can be easily made by the conditional density function. Therefore, Bayes decision rule is to choose the class with maximum $p(x,c_i)$ among n number of joint probability densities of the feature vector x.

$$x \in c_i \quad If \quad p(x,c_i) = Max\{p(x,c_1), \text{------}, p(x,c_n)\} \tag{5-2}$$

where

$p(x,c_i)$: joint probability density of pattern x and class i

When the density functions associated with the feature vectors are assumed to be Gaussian, conditional probability density function can be estimated by the equation (5-3).

After estimating mean and covariance for each class, the general multidimensional Gaussian density [42] for feature vector x with $2m$-dimensional functions is expressed as

$$p(x \mid c_i) = ((2\pi)^{(2m)/2} \mid \sum_i \mid^{1/2})^{-1} \exp[-0.5(x-\mu_i)^t \sum_i^{-1} (x-\mu_i)] \qquad (5\text{-}3)$$

where x : 2m-dimension feature vector

μ_i : 2m-dimension mean vector of class i

$\sum_i$: 2m by 2m covariance matrix of class i

$| \sum_i |$: determinant of $\sum_i$ of class i

C. Bayes Classifier in Security Study

1. The Feature Vector

The security assessment under a certain operating condition can be defined by its load variation. In this Chapter, system load is selected by random sampling from an assumed normal distribution function. According to the variation of system load, the system operating points moves to a new location with new load. The system operating status can be represented in different ways such as voltage magnitude and angle, real and reactive power of each bus or real and reactive power of transmission lines etc.. Since real and reactive powers in transmission lines vary over a wide range compared with voltage magnitude and angle, they are selected as parameters of the feature vector. The ith feature vector corresponding to system operating status with m transmission lines can be represented as

$$X_i = [\, P_{1,i} \text{ --- } P_{k,i} \text{ -----} P_{m,i}\, Q_{1,i} \text{ --- } Q_{k,i} \text{---- } Q_{m,i}\,]^T \qquad (5\text{-}4)$$

Where

$P_{k,i}$: Real power of transmission line k in the i th feature vector

$Q_{k,i}$: Reactive power of transmission line k in the i th feature vector

The selection of the feature vector in Baysian classifier has great influence on classification accuracy. In power system security analysis, it is impossible to store all

possible contingency cases with load variation. The suitable selection of feature vectors, therefore, is one of the important factors in the success of the Bayes classifier. In the power system security study, feature vectors should reflect various types of system operating status. The types of feature vectors are defined as a base case, single line or a generator contingency and double contingency etc. The base case is the case without generator or transmission line outage.

The number of feature vectors also plays an important role in Bayes classifier. With more feature vectors used for obtaining the distribution, the classification accuracy may be better but more computation effort is needed for characterization of a feature vector. The characterization of a feature vector is explained in detail in the next section.

2. Characterization of the Feature Vector

As shown in Chapter III, the characterization of system states in static security assessment requires the evaluation of post contingency steady state. For successful operation, a system should supply system load without the violation of operating conditions and load shedding in steady state. The optimal power flow (OPF) is performed under the constraints such as the limit of power flow and power generation for a contingency.

If the system has any problem such as load shedding or voltage instability, it is in emergency state. A feature vector corresponding to emergency state belongs to “group-zero” If all equipment and operating constraints are within their limits, the feature vector under these conditions is defined “group-one” in this Chapter. When there are n feature vectors in “group-one” (X^1) and o feature vectors in “group-zero” (X^o), these can be arranged as follow:

$$X^1 = [\, X_{1,} \text{ - - - - - - },X_n \,] \tag{5-5}$$

$$X^o = [X_{1+n}, \text{ - - - - - - },X_{o+n} \,] \tag{5-6}$$

3. Classification and Testing of Feature Vectors

In the last section, feature vectors are assigned as group-one or group-zero. The parameters of feature vectors for each group should be assumed to have a particular probability function. In this Chapter, Gaussian function is implemented as the probability density function of each parameter. If the parameter histogram of feature vectors for a group is far from a Gaussian function, the feature vectors should be separated into subclasses of a group. The dimension of the mean vector for each group is the same as that of the feature vector. When a group without subclasses has n feature vectors, the mean vector and covariance matrix are given by the equation (5-7) and (5-8) respectively.

$$M = [M_1 \text{ --- } M_k \text{ ---- } M_m \;\; M_{m+1} \text{ ---} M_{m+k} \text{ ---- } M_{2m}]^T \tag{5-7}$$

where

$$M_k = \frac{\sum_{i=1}^{n} P_{k,i}}{n}, \qquad M_{m+k} = \frac{\sum_{i=1}^{n} Q_{k,i}}{n}$$

n : the total number of feature vectors

m : the number of transmission lines

M_k : the real power average of k th element of feature vectors

M_{m+k} : the reactive power average of k th element of feature vectors

$P_{k,i}$: Real power of transmission line k in the i th feature vector

$Q_{k,i}$: Reactive power of transmission line k in the i th feature vector

$$S_{(2m,2m)} = \begin{bmatrix} S_{1,1} & S_{1,2} & - & S_{1,2m} \\ S_{2,1} & S_{2,2} & - & S_{2,2m} \\ | & | & \backslash & | \\ S_{2m,1} & S_{2m,2} & - & S_{2m,2m} \end{bmatrix} \tag{5-8}$$

where

$$S_{j,k} = S_{k,j} = \frac{\sum_{i=1}^{2m} (X_{i,j} - M_j)(X_{i,k} - M_k)}{2m}$$

$X_{i,j}$: i th element of the feature vector X_j

Here, covariance matrix describes the interrelationship between elements of feature vectors. It can be used for multidimensional distribution shown in the equation (5-3). Since feature vectors are selected by random sampling based on Gaussian function, the parameter function of a certain contingency type may be Gaussian too. The separation by every contingency type may lead to many subclasses. Once the average of feature inputs for each contingency type is computed, similar feature inputs based on their Euclidean distances are clustered. The number of subclasses is an important parameter for classification. When a group with *t* subclasses is considered, the general form of the mean vector is given by the equation (5-9). Covariance vectors for a group with *t* subclasses consist of *t* number of covariance vectors in the form of the equation (5-8).

$$M_{(2m,t)} = \begin{bmatrix} M_{1,1} & - & M_{1,s} & - & M_{1,t} \\ | & \backslash & | & \backslash & | \\ M_{k,1} & - & M_{k,s} & - & M_{k,t} \\ | & \backslash & | & \backslash & | \\ M_{m,1} & - & M_{m,s} & - & M_{m,t} \\ M_{m+1,1} & - & M_{m+1,s} & - & M_{m+1,t} \\ | & \backslash & | & \backslash & | \\ M_{m+k,1} & - & M_{m+k,s} & - & M_{m+k,t} \\ | & \backslash & | & \backslash & | \\ M_{2m,1} & - & M_{2m,s} & - & M_{2m,t} \end{bmatrix} \qquad (5\text{-}9)$$

where

$$M_{k,s} = \frac{P_{k,a+1} + P_{k,a+2} + - - - + P_{k,a+b-1} + P_{k,a+b}}{b}$$

$$M_{m+k,s} = \frac{Q_{k,a+1} + Q_{k,a+2} + - - - + Q_{k,a+b-1} + Q_{k,a+b}}{b}$$

k : *k* th parameter of the feature vector

a : the number of last element of the *k* th parameter vector in the (*s-1)* th subclass

b : the dimension of the *k* th parameter vector in the *s* th subclass

The procedure for the off-line process of Bayes classifier is as follows.

Step1 : Select the level of system load by random from Gaussian function. A feature vector is decided by the level of system load and a contingency. The active and reactive power of transmission lines is selected as feature vectors.

Step2 : Perform state characterization of feature vectors, which can be classified as group-one and group-zero. A group is able to have several subclasses.

Step3 : Obtain the mean and variance of feature vector elements for each subclass or group.

After obtaining the mean and variance of each subclass or group, the Bayesian decision rule is ready to be applied for the operating decision in power systems. With a given a new sampled feature vector, the classes are sorted by the conditional probabilities calculated with the Bayes' rule. The testing procedure for a new feature vector is described in following steps.

Step 4 : Obtain a new feature vector consisting of the real and reactive power through monitoring operating status.

Step 5 : The conditional probabilities are calculated based on the Bayes' rule in the equation (5-3). For convenience, applying a log on the decision function makes the equation (5-3) simplify. Since the dimension of feature vectors for the comparison of the decision function is always the same, first right part of the equation ($-m\log(2\pi)$) can be omitted. The Bayes decision function is rewritten in the equation (5-10).

$$g_i(x) = -\frac{1}{2}\log|\Sigma_i| - \frac{1}{2}(x-\mu_i)^t \sum_i^{-1}(x-\mu_i) \tag{5-10}$$

Step 6 : On the basis of the maximum value of the Bayes decision function, the feature vector is classified as group one or zero. For the Bayesian decision with a subclass k, given a feature vector x is

$$x \in c_i \quad \text{if} \quad g_i(x) = \max_{j=1,\cdots,k} g_j(x)$$

$$x \in \begin{cases} G_1 & \text{if } c_i \in G_1 \\ G_0 & \text{if } c_i \in G_0 \end{cases} \tag{5-11}$$

where

c_i : subclass i for classification of feature vectors

G_1 : group-one without any system problem

G_0 : group-zero with any system problem

After a feature vector under decision is tested in every subclass using equations (5-10) and (5-11), subclass of the feature vector is decided. If the subclass belongs to group-zero, the new operating statue has a system problem. Otherwise, a system is in normal or alert state in which all equipment and operation constraints are within their limits.

D. Case Study

The Western System Coordinating Council (WSCC) 3-machine, 9-bus system [12] is shown in Chapter III. The base MVA is 100 and system frequency is 60 Hz. The parameter and thermal limit of transmission lines are shown in Chapter III.

Table XVII. Example of State Characterization for Contingency Type

Contingency type	Result
Base case	Group-one
One Generator outage (G1,G2,G3)	Group-zero
One line outage(T1,T2,T3,T4)	Group-zero
One line outage(T5,T6,T7,T8,T9)	Group-one
One generator outage +One line outage	Group-zero
One generator outage +One line outage	Group-zero

An example of contingency types with load levels of 125, 90, and 100 are shown in Table XVII. This state characterization results from optimal power flow for load shedding minimization and voltage instability. For example, the outage of transmission lines (T4) results in voltage instability, leading to group-zero.

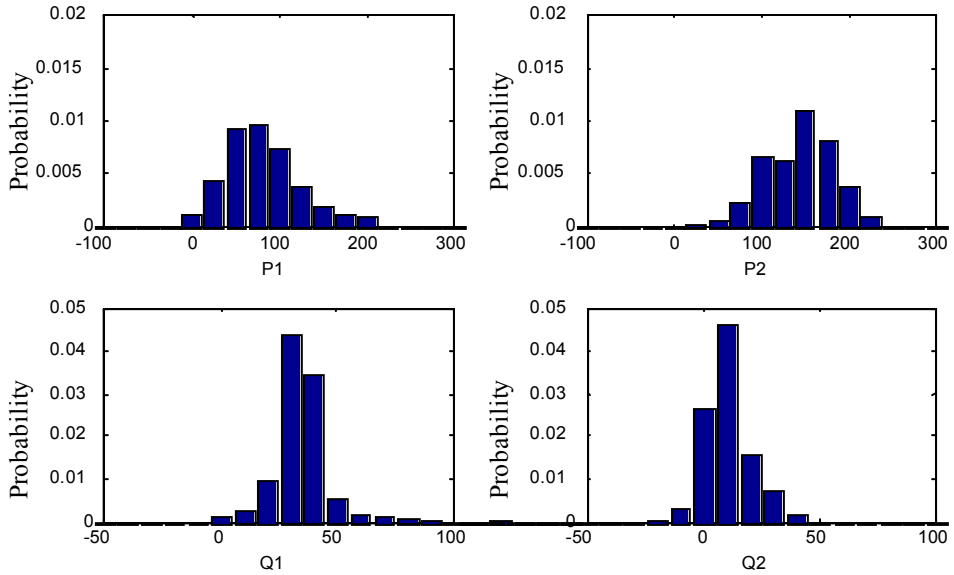

Fig. 12. The Histogram of Feature Vectors with Group-One (P1, P2, Q1 and Q2)

Although there are several elements in the feature vectors of group one, only *P1,* P2*, Q1,* and *Q2* parameters of feature vectors that belong to group-one for reasons of space limitations are shown in Fig. 12. Even though the histogram of feature vectors is not an exact Gaussian function, the mean and covariance matrix is calculated assuming a Gaussian function.

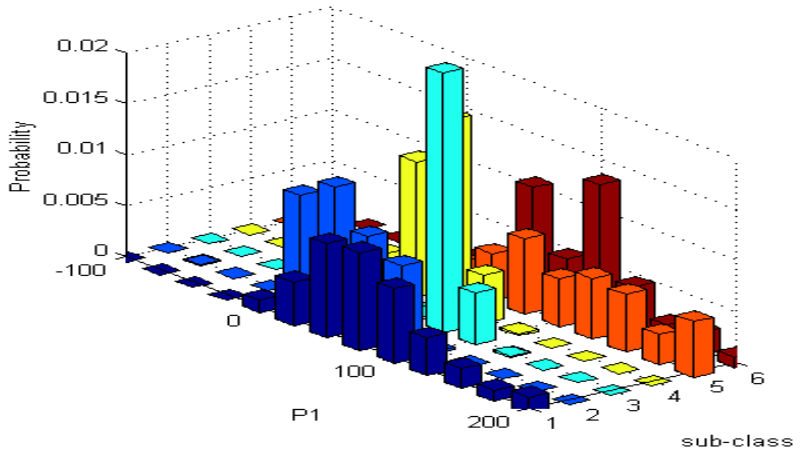

(a) The Histogram of P1 for Each Subclass

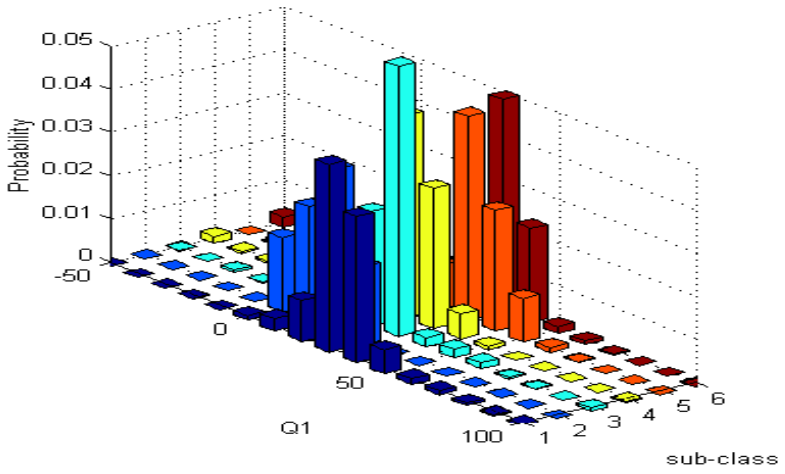

(b) The Histogram of Q1 for Each Subclass

Fig. 13. The Histogram of Parameters (P1, Q1) in Feature Vectors
(Group-one: subclass 1, Group-zero: subclass 2-6)

Since the parameter histogram of feature vectors for group-zero is far from a Gaussian function, the feature vectors are separated into 5 subclasses as shown in Fig. 13.

The classified feature vectors have their mean and covariance matrix. Table XVIII shows the mean vector of each subclass for Bayes decision function. Here, the covariance matrix is omitted.

A given feature vector can now be tested with the equation (5-10) and (5-11). The classification rate of Bayes classifier is compared with that of Self-Organizing Maps. Out of 7200 feature vectors including new feature vectors, only 57 sampling data is misclassified in Bayes classifier. Self-Organizing maps consist of 368 neurons with the same feature vectors. The results are shown in Table XIX.

Table XVIII. The Mean Vector of Subclasses

		P1 Q1	P2 Q2	P3 Q3	P4 Q4	P5 Q5
Group -one	Subclass 1	83.0667 34.5475	143.387 10.3622	90.6687 -0.1917	56.9564 23.8189	25.5819 12.2292
Group -zero	Subclass 2	34.0648 15.0254	142.207 1.4302	53.3019 -6.7161	22.4629 16.1995	7.4927 6.6065
	Subclass 3	64.6934 26.3776	64.5409 1.1412	123.612 -3.5761	63.5211 26.7872	1.409 6.6439
	Subclass 4	42.3753 21.8608	178.513 14.8871	65.8487 -7.3335	-0.2195 9.7122	42.3934 17.1939
	Subclass 5	1 19.18 33.6497	128.661 15.1791	73.4679 2.8210	106.323 26.3336	12.0857 2.5293
	Subclass 6	91.4927 26.4605	134.769 24.2652	99.4664 11.4899	2.684 6.5069	87.7713 15.9363
		P6 Q6	P7 Q7	P8 Q8	P9 Q9	
Group -one	Subclass 1	-67.673 0.6901	-64.5852 3.5492	74.4349 7.5379	-24.7533 -6.4874	
Group -zero	Subclass 2	-62.277 -2.9615	-34.5237 -0.0227	80.5107 6.5153	-10.5382 -8.9565	
	Subclass 3	-37.927 -1.9960	-48.6879 2.3514	4.9068 4.2647	-74.1322 -10.2685	
	Subclass 4	-126.02 -8.2788	-48.2991 3.6181	49.6586 -1.9262	-16.8407 -4.7455	
	Subclass 5	-19.600 2.1175	-79.4499 -4.2759	108.353 13.9447	7.4896 -1.1533	
	Subclass 6	-125.76 -14.379	-3.5839 0.3976	6.0477 -1.7408	-95.0281 -10.9994	

Table XIX. The Classification Rate of a Proposed Method

	Proposed Method	Self-Organizing Map
Classification rate	99.2%	98.1%

E. Summary

A method for security assessment employing the Bayes classifier is proposed in this Chapter. This method can be useful for system operators to make security decisions in on-line power system operation. Through an example of the WSCC system, the Bayes classifier shows how the power system operating condition can be classified. The results indicate that the classification rate of the Bayes classifier is 99.2%, which is a little better than that of Self-Organizing Maps in this study.

CHAPTER VI

CONSIDERATION OF THE RELIABILITY BENEFITS IN PRICING TRANSMISSION SERVICES

A. Problem Formulation

The embedded costs of transmission transactions are usually the largest component of the total transaction cost. The embedded cost methodologies [44, 45] have not fully included reliability benefits, which is reliability based on transmission charge while pricing transmission services. References [46, 47] emphasize the importance of reliability benefits to recover the true value of embedded costs. This method, however, can be improved.

The embedded costs can be taken into account by a combination of two parts, allocation based on capacity-use and allocation based on reliability benefits. However, the portion of each allocation can be changed by the ratio of these two parts. There is no established rule to assign the ratio between these two components.

The transmission line capacity in an actual power system is an important factor. Therefore, reliability benefits in pricing transmission transaction costs should be computed under the constraint of transmission line capacity.

In this Chapter, we shall first consider reliability benefits under the constraint of transmission line capacity and then show how to combine allocation based on transmission line capacity-use and allocation based on reliability benefits. We shall describe how to calculate the ratio between capacity-use and reliability benefits based on a reliability index. We also look at reliability benefits when transmission line capacity is considered. We then review the example presented in [46] and discuss the use of transmission transaction costs.

B. Description of a Pricing Method

Most of the traditional approaches in defining transmission transaction costs ignore reliability cost/worth. To get equitable and reasonable transmission transaction costs for both customers and power suppliers, it is desirable that pricing should reflect reliability cost. Since the embedded costs for using transmission facilities, such as transformers and transmission lines, are generally large, this Chapter focuses only on embedded costs in total transmission transaction cost. When considering reliability cost, embedded costs are composed of two parts: allocation based on capacity-use and allocation based on reliability benefits. Hence, the total embedded cost can be expressed as:

Embedded cost = Capacity-use + Reliability benefits

Here, the buyers do not pay any additional cost as reliability cost. The total embedded cost is the same as they are when not considering reliability cost, because the total embedded cost is a fixed charge.

For allocation based on capacity-use, an AC power flow algorithm based on a MW-mile method [46, 48] is implemented in this Chapter. This method allocates the charges for each wheeling participant based on the use of existing transmission facilities. This method is simple to understand and to apply to real power systems. The impact on system reliability depends on pricing methods. The MW-mile method provides better system reliability than the other methods due to inherent mechanism of discouraging long distance transactions. Since capacity-use is determined by amount of transmitted power and transmission line length, this method gives us satisfactory results. The capacity-use component of embedded cost of transmission line j for transaction *Ti* is defined in the equation (6-1).

$$C_{j;Ti} = \left[\frac{MW_{j;Ti} \bullet L_j \bullet f_j}{\sum_i MW_{j;Ti}} \right] \qquad (6\text{-}1)$$

where

$MW_{j;Ti}$: The power transmitted in line *j* for transaction T_i.

L_j : The length of the line *j*.

f_j : The cost per unit transmission line length.

Meanwhile, embedded costs based on reliability benefits allocate the charge for each wheeling participant by the reliability index for each transaction. It's computed as the difference of probability of system failure when all lines are up and when only line j is down. Fig. 14 shows a flowchart for the reliability benefits calculation of line *j* for each transaction. It is similar to the capacity-use equation after computing difference of probabilities of system failure.

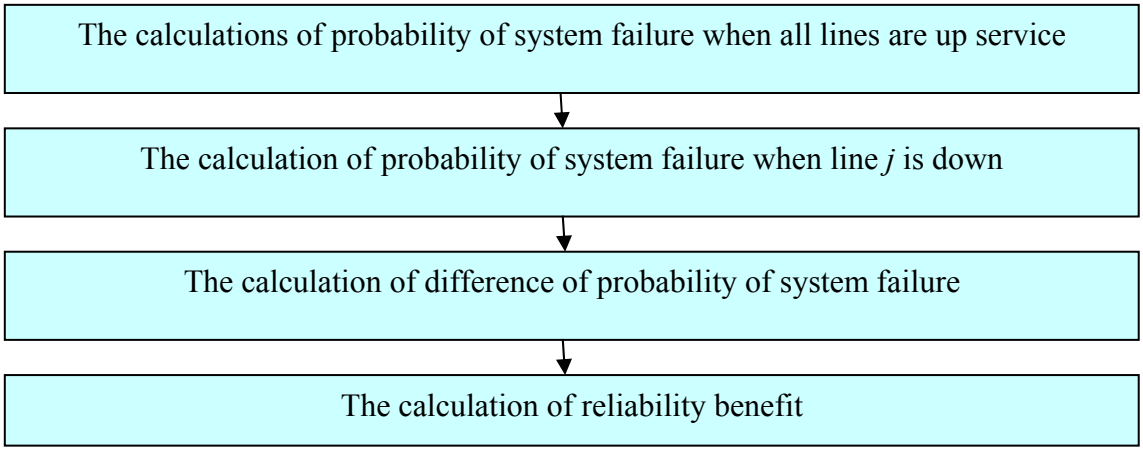

Fig. 14. A Flowchart for the Reliability Benefits Calculation

The embedded cost of the transmission line *j* allocated to transaction *Ti* based on reliability benefits is formulated as the equation (6-2).

$$RB_{j;Ti} = \left[\frac{R_{j;Ti}}{\sum_i R_{j;Ti}} \right] \bullet L_j \bullet f_j \qquad (6\text{-}2)$$

where

$R_{j;Ti}$: The reliability benefits for line *j* for transaction *Ti*

The total embedded cost of capacity-use and reliability benefits can be expressed as the sum of equations (6-1) and (6-2). The ratio between these is explained in the following section in detail.

1. The Relationship of Capacity-use and Reliability Benefits

Capacity-use and reliability-benefits of transmission line *j* are expressed separately. This section describes how to combine capacity-use and reliability benefits. The problem is to allocate a portion of the total embedded cost to reliability benefits, because the total embedded cost should not be changed. If the ratio between capacity-use and reliability benefits depends on an expert's decision, the ratio problem of transmission transaction cost allocation can be a matter of dispute. The ratio should then be decided not by an individual's opinion but by the probability of system failure. If a system has very high reliability, reliability benefits don't need to be considered in calculation of embedded costs. If a system has very low reliability, reliability benefits should occupy a large portion in the computation of embedded cost.

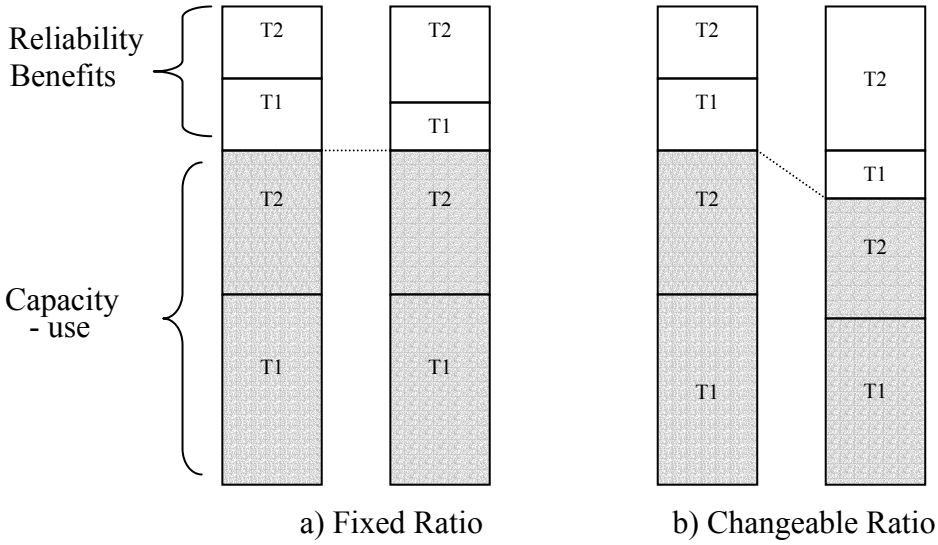

Fig. 15. An Example of Each Transaction Portion According to the Probability of System Failure

An example of embedded cost portion for each transaction is shown in Fig. 15. As shown in Fig 15-(a), embedded costs of all transactions can't be changed in allocation of capacity-use as well as in allocation of reliability benefits when the ratio is fixed by an individual opinion. Only the portion of embedded costs for each transaction can be changed in both capacity-use and reliability benefits. The portion of reliability benefits for each transaction can be varied by the change of line parameter such as transmission line availability and transmission line capacities. For example in Fig 15-(a), the portion of reliability benefits for transaction *T2* is increased while the portion of reliability benefits for transaction *T1* is decreased. They then have a trade-off relationship due to the fixed ratio. Even though both transactions worsen system reliability, transaction *T1* can charge much less for its responsibility.

Fig 15-(b) denotes the change of ratio according to the probability of system failure. Now, suppose that the portion of transaction *T1* and transaction *T2* in both reliability benefits and capacity-use is the same as in Fig. 15-(a) even though the ratio is changed. Because the portion of reliability benefits in the total embedded cost is increased, reliability benefits for both transaction *T1* and *T2* become larger than those of Fig. 15-(a). It means this transaction has more responsibility to pay according to the system reliability.

The proposed method based on the probability of system failure *P(SF)* then is more reasonable and effective than adjusting by each individual's opinion in solving the ratio between capacity-use and reliability benefits. The analytical method is used in order to solve the probability of system failure. The probability of total system failure can be expressed as in the equation (6-3).

$$P(SF) = \sum_{i=1}^{n} (P_{Ti} \bullet P(SFi)) \qquad (6\text{-}3)$$

where $P(SF_i)$ is the probability of sytem failure for transaction *Ti* and P_{Ti} is the probability of occurrence for transaction *Ti.*

The embedded costs allocated to transaction T_i based on reliability benefits and capacity-use are expressed as follows.

$$RB_{Ti} = P(SF) \bullet \sum_j RB_{j;Ti}$$
$$C_{Ti} = (1 - P(SF)) \bullet \sum_j C_{j;Ti} \quad (6\text{-}4)$$

The parameter of capacity-use is $1 - P(SF)$, while that of reliability benefits is $P(SF)$. The sum of those is the total embedded cost. The transmission transaction does not actually affect any new transmission costs. The embedded costs of each transaction (S_{Ti}) are

$$S_{Ti} = \sum_j C_{j;Ti} - P(SF)(\sum_j C_{j;Ti} - \sum_j RB_{j;Ti})$$
$$= C_{Ti} + RB_{Ti} \quad (6\text{-}5)$$

From the equation (6-5), the embedded cost allocated to transaction T_i depends on the probability of system failure, the portion of capacity-use and the portion of reliability benefits. When the probability of system failure is zero, reliability benefits cannot affect the total embedded cost. It means the total embedded cost is only for capacity-use. Capacity-use also cannot influence the total embedded cost when probability of system failure is one.

The total embedded cost of all transactions is the sum of each transaction. Therefore, the total embedded cost (S_T) is

$$S_T = \sum_i S_{Ti} \quad (6\text{-}6)$$

The computation of embedded cost is formulated by equations in this section. When considering the change of transmission line capacities, embedded costs of both reliability benefits and capacity-use may be changed for each transaction.

2. Embedded Costs Under Line Capacity Constraints

In an actual power system, transmission lines have their capacities along with the probability of availability. Line flow should not exceed these capacities. The maximum flow in a network can be obtained by a max-flow algorithm [49] used with a network representation from a given source node (S) to a sink node (N) under constraints of transmission line capacities. This approximation, which relies only on Kirchhoff's first law, may be suitable for this application to power systems. A simple network for transactions is shown in Fig. 16.

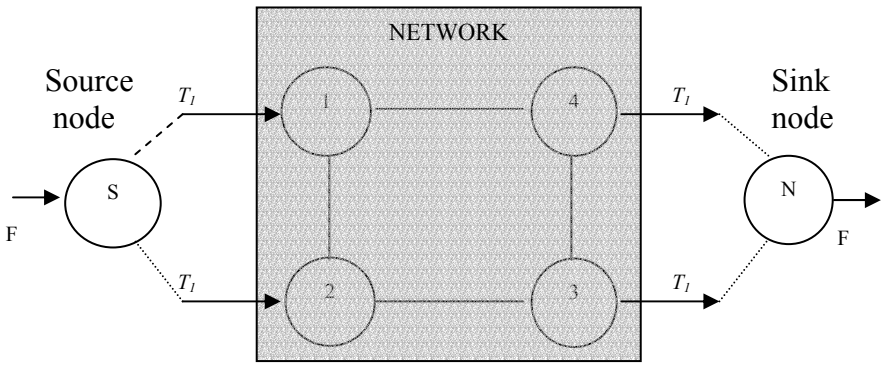

Fig. 16. A Simple Network with Capacities for Transactions.

In power system network analysis, a transaction *T1* is one of the cases, where a power utility that owns several generating plants sells power to several buyers. The sum of flow into node 1 and 2 is the total flow of a transaction (*T1*), which is the total supply of power from the seller. It should be equal to the sum of flow out of node 3 and 4. If not, this transaction may be failed. The problem of maximal flow calculations is expressed as follow:

$$\text{Maximize} : F = \sum_{j=1}^{n} x_{Sj} \tag{6-7}$$

$$\text{Subject to} : \sum_{j=1}^{n} x_{Sj} - \sum_{j=1}^{n} x_{jS} - F = 0$$

$$\sum_{j=1}^{n} x_{Nj} - \sum_{j=1}^{n} x_{jN} + F = 0$$

$$\sum_{j=1}^{n} x_{ij} - \sum_{j=1}^{n} x_{ji} = 0, \quad (\ i \neq S, N \quad i = 1,\text{-----},n)$$

$$0 \leq x_{ij} \leq C_{ij}, \quad \text{all } i, j$$

where F : The total flow of a transaction

x_{ij} : The line flow from node *i* to node *j* (S : source node, N : sink node)

C_{ij} : The line capacitor of from node *i* to node *j*

The purpose of maximum flow calculations for each transaction is to determine whether or not the transaction is possible. When the total required line flow for each transaction is larger than maximum flow in a network, the probability of system failure is one.

Capacity-use for any transaction is changed according to transmission line capacities. An AC OPF program under the constraints for transmission line capacities computes capacity-use. Since the transmitted power of each transmission line is different due to transmission line capacities, capacity-use for each transaction is also changed.

Reliability benefits for any transaction are calculated as the difference of the total probability of system failure. The process of the reliability benefits computation itself is similar to a conventional method as described before in this Chapter. The considerations of transmission line capacities, however, make the computation of reliability benefits complicated.

The sensitivity of reliability benefits shows that the transaction affects reliability benefits by the change of transmission line capacities. The sensitivity of reliability benefits is taken into account by the difference of each transaction as follow.

$$Senstivity \quad = \Delta RB_{Ti} \tag{6-8}$$

For example, suppose that the embedded costs of reliability benefits for a particular transaction are increased and embedded costs of reliability benefits for the others are almost the same when the transmission line capacities are changed. This transaction has the responsibility to charge more.

The proposed approach is explained explicitly in the flowchart as shown in Fig. 17.

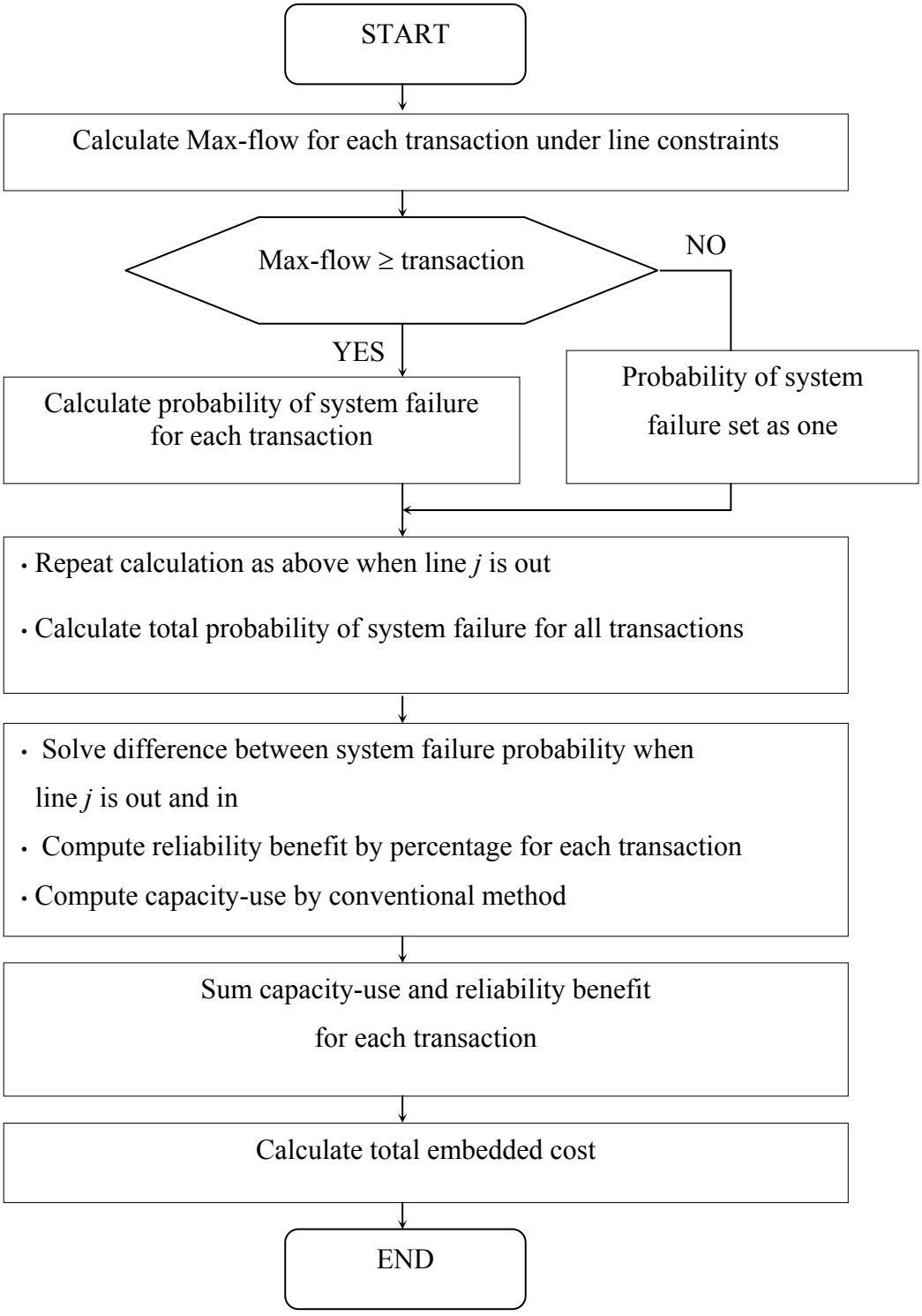

Fig. 17. A Flowchart for the Proposed Pricing Method

C. Numerical Example

Fig. 18 shows a simple eight-bus system for embedded cost study as used in [46]. All data of this system are shown in Table XX. In transaction *T1*, utility company owns generators and several loads. Transaction *T2* and transaction *T3* are wheeling transactions. The probability of occurrence for each transaction is assumed the same. The cost function of bus 1 and bus 2 are *0.01P2+10P* and *0.08P2+5P* respectively.

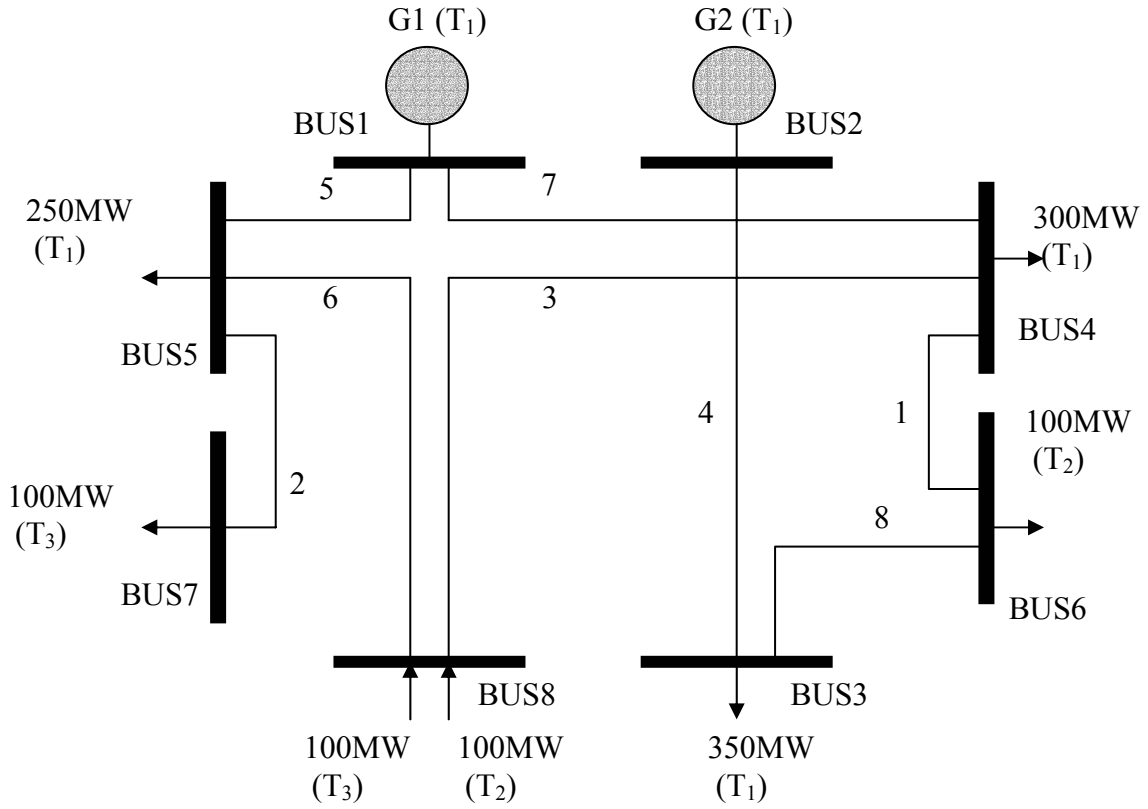

Fig. 18. One Line Diagram of Eight-Bus System

Table XX. The Data of Eight-Bus System

(a) Transmission Line Data

No. of Line	R(p.u.)	X(p.u.)	L(km)	P. O. A.
1	.015	.045	300	0.9
2	.005	.015	100	1.0
3	.015	.045	300	0.9
4	.015	.045	300	0.9
5	.005	.015	100	1.0
6	.005	.015	100	1.0
7	.015	.045	300	0.9
8	.005	.015	100	0.9

P.O.A. : probability of availability

(b) Transaction and Generation Data

Transaction	From	To
T1	G1 : 1000 [MW rating] G2 : 600 [MW rating]	Bus 3 : 350 [MW] Bus 4 : 300 [MW] Bus 5 : 250 [MW]
T2	Bus 8 : 100 [MW]	Bus 6 : 100 [MW]
T3	Bus 8 : 100 [MW]	Bus 7 : 100 [MW]

Power factor : 0.86

(c) Probability of Occurrence for Each Transaction

Transaction	Probability (%)
T1	1/3
T2	1/3
T3	1/3

As shown in Fig. 19, an example of Fig. 18 can be simplified. The number in the circle represents a bus number. Since the probability of line availability of line number 2, 5 and 6 is one, those lines is not considered. The lines between bus 3 and 4 is expressed as line 18. The first one and second one in parenthesis are transfer power and line capacities respectively.

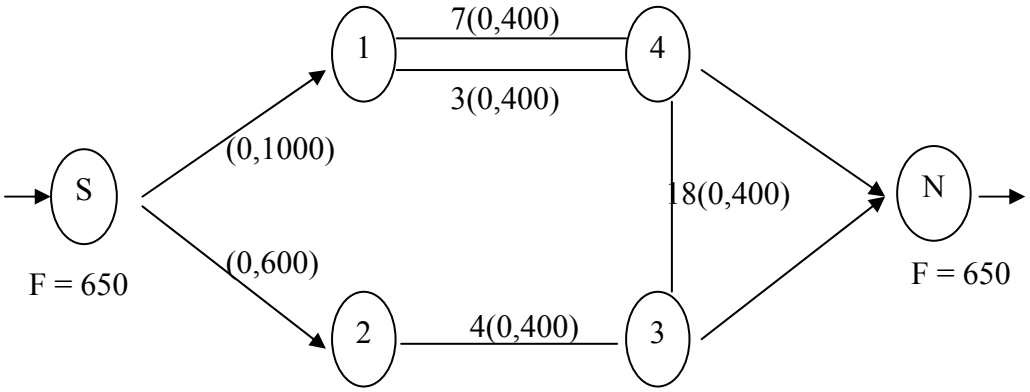

Fig. 19. A Simplified Model of Transaction *T1* for Maximum Flow

When a transmission capacity for each line is 400 [MW], the probability of system failure for transaction *Ti* with all lines *P(SFi)* can be calculated by state transition diagram as shown in Fig. 20. For example, cases such as case 6, 7, 9, 11, 12, 13, 14 15 and 16 cause a system failure, which means the power of sending node can not be deliver the sink node. The sum of the probability of these cases is the probability of system failure for transaction *Ti*.

To get reliability benefits, the probability of system failure is shown in Table XXI-(a) when only line *j* is out or down. The probability of system failure without line *j* can be computed in the same manner as the probability of system failure with all lines. *P(SF j,i)* is the probability of system failure for transaction *Ti* when only line *j* is out. *P(SFi)* is the probability of system failure for transaction *Ti* with all lines. The difference between *P(SF j,i)* and *P(SFi)* has an important meaning. From this table, *P(SF 5,1)* - *P(SF1)* is largest value and transmission line 5 has the most crucial role in transaction *T1*. Table XXI-(b) presents the percentage of reliability benefits for each transaction when

transmission line *j* is down. It can be seen that when line 4 or line 8 is down, transactions *T2* and *T3* of line 4 or 8 do not affect reliability benefits.

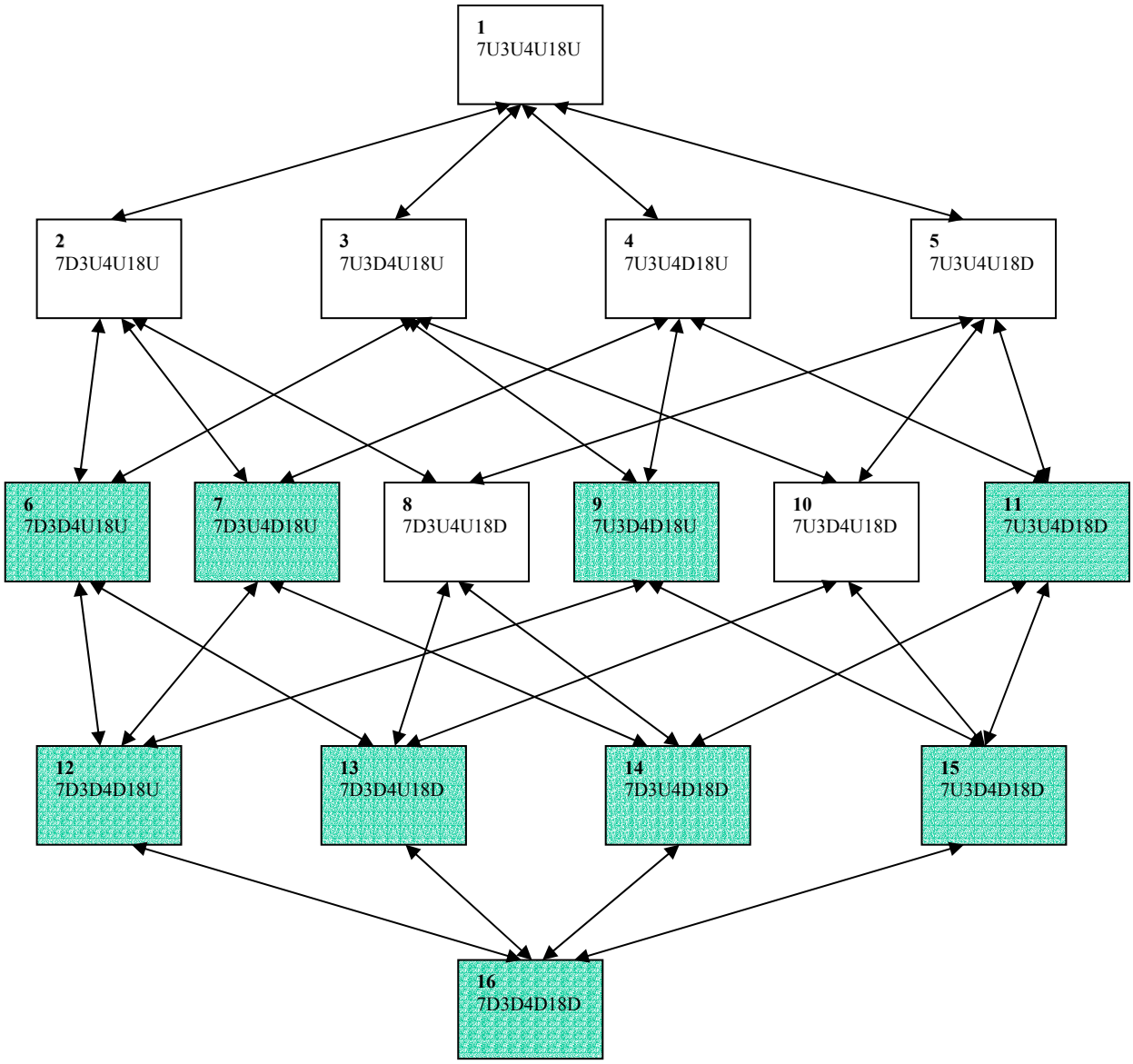

Fig. 20. State Transition Diagram of Eight-Bus System

Table XXI. The Probability of System Failure and Percentage of Reliability Benefits

(a) The Probability of System Failure without the Transmission Line j *P(SF j,1)* and Difference of Probability of System Failure *P(SF j,1) - P(SF1)* according to Transmission Line Change in Transaction *T1*.

Line No. *j*	Capacity = 700 [MW]		Capacity = 400 [MW]	
	P(SF *j*,1)	P(SF *j*,1) - P(SF1)	P(SF *j*,1)	P(SF *j*,1) - P(SF1)
1	0.109	0.08019	0.109	0.06561
2	0.02881	0.0	0.04339	0.0
3	0.1172	0.08839	0.01901	0.14671
4	0.0613	0.03249	0.3439	0.30051
5	0.729	0.70019	1	0.95661
6	0.1172	0.08839	0.01901	0.14671
7	0.1172	0.08839	0.01901	0.14671
8	0.109	0.08019	0.109	0.06561

(b) The Percentage of Reliability Benefits for Each Transmission Line in Each Transaction

Line No. *j*	Capacity = 700 [MW]			Capacity = 400 [MW]		
	T1	T2	T3	T1	T2	T3
1	8.25	91.74	0	6.86	93.14	0
2	0	0	100.0	0	0	100.0
3	52.18	47.82	0	64.63	35.57	0
4	100.0	0	0	100.0	0	0
5	89.63	10.37	0	92.19	7.81	0
6	24.59	22.54	52.87	35.12	19.39	45.49
7	52.18	47.82	0	64.43	35.57	0
8	100.0	0	0	100.0	0	0

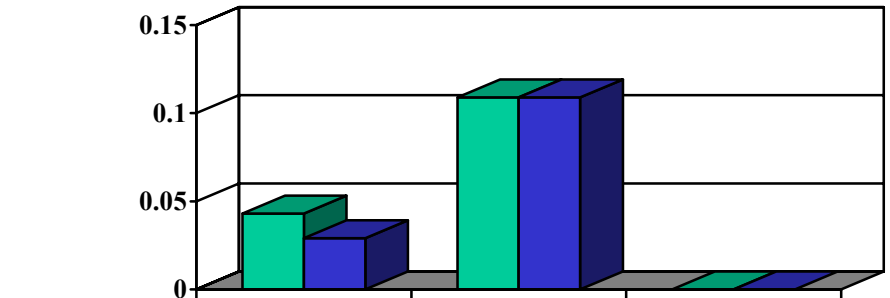

	P(SF1)	P(SF2)	P(SF3)
capacity=400	0.043	0.109	0
capacity=700	0.029	0.109	0

Fig. 21. The Probability of System Failure with Line Capacity Change

The probability of system failure for each transaction according to transmission line capacity change is shown in Fig. 21. When transmission line capacities are increased, the probability of system failure in transaction *T1* is also increased. The probability of system failure in transactions *T2* and *T3* is constant because these two transactions transmit only 100 [MW]. Total probability of system failure is 0.051 by the equation (6-3) when transmission line capacities are 400 [MW].

Table XXII-(a) is the result of the proposed approach including only capacity-use, only reliability benefits, and capacity-use plus reliability benefits according to transmission line change. When transmission line capacities are decreased from 700 [MW] to 400 [MW], the total percentage of reliability benefits is 4.6 and 5.1 respectively due to the probability of system failure. For transaction *T1*, reliability benefits are increased because this transaction worsens system reliability. Hence, embedded costs of reliability benefits for transaction *T1* become higher than other transactions due to sensitivity of reliability benefits. The sensitivity of reliability benefits for transactions *T2* and *T3* is almost zero.

Table XXII-(b) shows the comparison of the proposed method and two conventional methods. Postage stamp (D) is not equitable because it ignores the actual system power flow. A conventional method (E) cannot explain transmission line capacity change in reliability benefit calculation even though reliability benefits are considered. Also, the portion of reliability benefits is so high that it occupies a large part of the total

embedded cost. Meanwhile, the portion of reliability benefits (4.6%) is more or less small in the proposed method compared with the conventional method (E). Also, the change of transmission capacities can be explained too.

Table XXII. The Embedded Costs of Proposed and Conventional Methods

(a)The percentage of embedded costs of (A) capacity-use, (B) reliability benefits and (C) capacity-use + reliability benefits according to the change of transmission line capacity

	Capacity = 700 [MW]			Capacity = 400 [MW]		
	A	B	C	A	B	C
T1	59.6	2.5	62.1	55.9	3.0	58.9
T2	23.6	1.7	25.3	27.4	1.7	29.1
T3	12.2	0.4	12.6	11.6	0.4	12.0
Total	95.4	4.6	100	94.9	5.1	100

(b) The percentage embedded costs of conventional method (D) postage stamp (E) capacity-use + reliability benefits with fixed ratio (0.8 : 0.2) and proposed method when transmission line capacity is 700MW.

	Conventional method		Proposed method
	D	E	
T1	81.8	60.7	62.1
T2	9.1	27.2	25.3
T3	9.1	12.1	12.6

D. Summary

This Chapter has described a procedure for allocating transmission transaction costs when considering reliability benefits. The consideration of reliability benefits contributes to allocation of transmission transaction costs more equitably.

In our proposed approach, we deal with reliability benefits according to the change of transmission line capacities. To decide success or failure of each transaction, a max-flow algorithm is employed. As explained through an example, the change of reliability benefits under constraints of transmission line capacities cannot be ignored.

Therefore, the calculation of reliability benefits should include constraints of transmission line capacities. We also showed the relationship of capacity-use and reliability benefits, which depends on the probability of system failure.

CHAPTER VII

CONCLUSIONS

A. Summary of the Research Contribution

This dissertation has presented new approaches for probabilistic security assessment and transmission pricing. The major contributions of the work developed in this dissertation can be summarized as follows:

- A probabilistic method is developed for power system security assessment by sequential Monte-Carlo simulation. This method takes into account dynamic and static effects, which can be included by transient stability, satisfaction of load without violation of constraints and voltage stability studies. In the alert state, the consideration of additional contingencies based on the system state probability deals with a probabilistic approach in a better manner. The probabilities and frequencies for operating states represent reliability security indices for security assessment, which can provide valuable information on system security. The analytical method and Monte-Carlo simulation are tested in the WSCC system. To demonstrate the efficiency of this approach, Monte-Carlo simulation is applied to the IEEE RTS with various system loads.
- Monte-Carlo simulation in security assessment requires a large amount of computation time due to state characterization for each sampled state. This problem can be overcome by combining Monte-Carlo simulation and Kohonen Networks. Data classification by SOM can reduce sampling data. The SOM-MCS reduces computation time for reliability security indices when using classified data. The LVQ-MCS can avoid the drawback of straight Monte-Carlo simulation that the characterization of sampled state is time consuming. The simulation results of both SOM-MCS and LVQ-MCS approaches in modified IEEE RTS have shown a reasonable accuracy and significant reduction of computation time.
- A Bayes classifier is proposed as a tool for static security assessment in power systems. This method can be useful for system operators to make security decisions

in on-line power system operation without a complicated contingency analysis in the testing stage. Security status of testing patterns including new feature vectors is determined by maximum a posteriori probability rule based on the Bayes rule. The proposed approach can contribute to improve on-line security assessment with accuracy as shown through the case study of WSCC system.

- A transmission pricing method is developed for allocating transmission transaction costs based on reliability benefits in transmission services. The proposed methodology shows how to allocate transaction costs of reliability benefits when transmission line capacity is considered. Moreover, the ratio between allocation by transmission line capacity-use and allocation by reliability benefits is calculated based on a reliability index. Under restructured environment, the number of transactions may be increased. This may result in worsening system reliability. Embedded costs should be considered not only by allocation based on transmission line capacity-use, but also by allocation based on reliability benefits. It provides useful information on the planning of transmission line expansion.

B. Suggestions for Further Studies

It may be possible to extend the studies presented in this dissertation in several directions. Some of recommendations are summarized as follows.

1) In security studies, there are several issues that need further investigation:

- In this dissertation, the dynamic behavior has been examined by transient stability. The evaluation of frequency drops following loss of a generator, multi-swing loss of synchronism, and voltage dynamics can also be investigated for including dynamic effects.
- Three-phase-fault has been assumed as the fault type in this dissertation. Including other fault types, based on statistical data, can be investigated for their effect on the computed stability index.
- In transient stability, bisection method has been implemented for the reduction of computation time. The development of faster and more powerful techniques can improve the computational efficiency.

2) The IEEE RTS has been used to indicate the efficiency of the proposed SOM-MCS and LVQ-MCS methods. In practice, probabilistic reliability and security evaluation methods are generally applied to reduced equivalent models or sections of systems that are of interest. However, further research needs to continue to increase its capability of methods to deal with large networks.

3) A Bayes Classifier has been implemented for operation in security assessment. Like SOM-MCS or LVQ-MCS, the combination of Monte-Carlo simulation with a Bayes classifier can be implemented for security evaluation.

4) This dissertation has presented a method for calculating contribution of reliability benefit in transmission service pricing. The inclusion of losses and reactive power aspects may still be required for equitable transmission pricing.

REFERENCES

[1] A. D. Patton, C. Singh, and D. G. Robinson, "The impact of restructuring policy changes on power grid reliability," Final Report, Project SAND98-2178, Sandia National Laboratories, Albuquerque, NM, Oct. 1998.

[2] N. Balu, T. Bertram, A. Bose, V. Brandwajn, G. Cauley *et al.*, "On line power system security analysis," *in Proceedings of IEEE,* vol. 80, no. 2, pp. 262-280, Feb. 1992.

[3] R. Billinton, "Composite system reliability evaluation," *IEEE Transactions on Power Apparatus & Systems*, vol. PAS-88, no. 4, pp. 276-281, Apr. 1969.

[4] C. Singh and R. Billinton, *System Reliability, Modeling and Evaluation*, London: Hutchinson, 1977.

[5] J. D. McCalley, V. Vittal, and N. Abi-Samra, "An overview of risk based security assessment," *in Proceedings of IEEE Power Engineering Society 1999 Summer Meeting*, vol. 1, pp. 173–178.

[6] J. D. McCalley, A. A. Fouad, V. Vittal, B. L. Irizarry-Rivera, and R.G Farmer "A risk-based security index for determining operating limits in stability-limited electric power systems," *IEEE Transactions on Power Systems*, vol. 12, no. 3, pp. 1210–1219, Aug. 1997.

[7] C. Singh, A. D. Patton, A. Lago-Gonzalez, A. R. Vojdani, G. Gross, F. F. Wu, and N. J. Balu, "Operating considerations in reliability modeling of interconnected systems-an analytical approach," *IEEE Transactions on Power Systems*, vol. 3, no. 3, pp. 1119–1126, Aug. 1988.

[8] C. Singh and Q. Chen "Modeling of energy limited units in the reliability evaluation of multi-area electrical power systems," *IEEE Transactions on Power Systems*, vol. 5, no. 4, pp. 1364–1373, Nov. 1990.

[9] S. Aboreshaid and R. Billinton, "A framework for incorporating voltage and transient stability considerations in well-being evaluation of composite power system," *in Proceedings of IEEE Power Engineering Society 1999 Summer Meeting,* vol. 1, pp. 219–224.

[10] A. M. Silva, J. Endrenyi, and L. Wang, "Integrated treatment of adequacy and security in bulk power system reliability evaluation," *IEEE Transactions on Power Systems,* vol. 8, no.1, pp. 275-285, Feb.1993.

[11] V. A. Levi, J. M. Nahman, and D. P. Nedic, "Security modeling for power system reliability evaluation," *IEEE Transactions on Power Systems*, vol. 16, no. 1, pp. 29–37, Feb. 2001.

[12] R. Billinton, and W. Li, *Reliability Assessment of Electric Power Systems Using Monte Carlo Methods*, New York: Plenum Pub Corp, 1994.

[13] H. H. Happ, "Cost of wheeling methodologies," *IEEE Transactions on Power Systems*, vol. 9, no. 1, pp. 147-156, Feb. 1994.

[14] H. Rudnick, R. Parma and J. E. Fernandez "Marginal pricing and supplement cost allocation in transmission open access," *IEEE Transactions on Power Systems*, vol. 10, no. 2, pp. 1125-1142, May 1995.

[15] Hyde M. Merrill and Bruce W. Ericson, "Wheeling rates based on marginal-cost theory," *IEEE Transactions on Power Systems*, vol. 4, no.4, pp. 1445-1451, Oct. 1989.

[16] Lester H. Fink and Kjell Carlsen, "Operating under stress and strain," *IEEE Spectrum* Mar. 1978.

[17] Tomas E. Dy Liacco, "The adaptive reliability control system," *IEEE Transactions on Power Apparatus and Systems,* vol. PAS-86, no.5, May 1967.

[18] M. Pavella and P.G. Murthy*, Transient Stability of Power Systems –Theory and Practice,* New York: John Wiley & Sons, 1994.

[19] V. Vittal, "Consequence and impact of electric utility industry restructuring on transient stability and small-signal stability analysis," *in Proceedings of the IEEE*, vol. 88, no.2, pp. 196–207, Feb. 2000.

[20] Y. Hsu and C. Chang, "Probabilistic transient stability studies using the conditional probability approach," *IEEE Transactions on Power Systems,* vol. 3, no. 4, pp. 1565–1572, Nov. 1988.

[21] R. Billinton and S. Aboreshaid, "Stochastic modeling of high-speed reclosing for probabilistic transient stability studies," *in IEE Proceeding Generation, Transmission and Distribution, Part C,* vol. 142, no. 4, pp. 350–354, Jul. 1995.

[22] S. Aboreshaid, R. Billinton and M. Fotuhi-Firuzabad, "Probabilistic transient stability studies using the method of bisection," *IEEE Transactions on Power Systems,* vol. 11, no. 4, pp. 1990–1995, Nov. 1996.

[23] X. Luo, C. Singh and A .D. Patton, "Loss-of-load state identification using self-organizing map," *in Proceedings of IEEE Power Engineering Society 1999 Summer Meeting*, vol. 2, pp. 670-675.

[24] P. Kessel and H. Glavitch, "Estimating the voltage stability of a power system," *IEEE Transactions On Power Delivery*, vol. 1, no. 3, pp. 346-354, Jul. 1986.

[25] S Aboreshaid and R Billinton, "Probabilistic evaluation of voltage stability," *IEEE Transactions on Power Systems,* vol. 14, no. 1, pp. 342-348, Feb. 1999.

[26] Peter W. Sauer and M. A. Pai, *Power System Dynamics and Stability*, Upper Saddle River, NJ: Prentice Hall, 1997.

[27] IEEE RTS Task Force of APM Subcommittee, "IEEE reliability test system," *IEEE Transactions on Power Apparatus and Systems*, vol. PAS-98, no. 6, pp. 2047-2054, Nov/Dec. 1979.

[28] L. L. Lai, *Intelligent system applications in power engineering*, New York: John Wiley & Sons, 1998.

[29] D. Neibur and A. Germond, "Power system static security assessment using Kohonen neural network classifier," *IEEE Transactions on Power Systems*, vol. 7, no. 2, pp. 865-872, May 1991.

[30] M. A. El-Sharkawi and R. Atteri, "Static security assessment of power system using the Kohonen neural network," *ANNPS'*93, Tokyo, Japan, pp. 373-377, Apr. 1993.

[31] H. Hori, Y. Tamaru and S. Tsuzuki, “An artificial neural-net based techniques for power system dynamic stability with the Kohonen model,” *IEEE Transactions on Power Systems*, vol. 7, no. 2, pp. 856-864, May 1992.

[32] T. Baumann, A. Germond, and D. Tschudi, “Impulse test fault diagnosis on power transformers using Kohonen’s self-organizing neural networks,” *in Proceedings of the 3rd Symposium on Expert System Applications to Power Systems*, Tokyo, Japan, pp. 642-647, Apr. 1991.

[33] A. Germond, N. Macabrey and T. Baumann, “Application of neural networks to load forecasting,” *in Proceedings of INNS-Summer Workshop "Neural Networks Computing for the Electric Power Industry,"* Stanford, CA, pp. 165-171, Aug. 1992.

[34] X. Luo, C. Singh and A. D. Patton, “Loss-of-load state identification using self-organizing map,” *in Proceedings of IEEE Power Engineering Society 1999 Summer Meeting*, vol. 2, pp. 670-675.

[35] SOM Toolbox Team Helsinki University of Technology, “Technical report on SOM toolbox 2.0,” April 2000.

[36] T. Kohonen, *Self-Organizing Maps*, Series in Information Sciences, vol. 30, New York: Springer, 1997.

[37] I. Kamwa, R. Grondin, L. Loud, “Time-varying contingency screening for dynamic security assessment using intelligent-systems techniques,” *IEEE Transactions on Power Systems*, vol. 16, no. 3, pp. 526–536, Aug. 2001.

[38] Ernan Ni and Peter B. Luh "Forecasting power market clearing price and its discrete PDF using a Bayesian-based classification method," *in Proceedings of IEEE Power Engineering Society 2001 Winter Meeting*, vol. 3, pp. 1518–1523.

[39] K. A. Clements, A. S. Costa and A. Agudelo, "Identification of parallel flows in power networks operating under deregulated environments," *in Proceedings of IEEE Power Engineering Society 2001 Summer Meeting*, vol. 1, pp. 434–438.

[40] Jun Zhang, Jian Pu, J. D. McCalley, H. Stern and W. A. Gallus "A Bayesian approach for short-term transmission line thermal overload risk assessment," *IEEE Transactions on Power Delivery*, vol. 17, no. 3, pp. 770–778, Jul. 2002.

[41] D. C. Yu, T. C. Nguyen, and P. Haddawy, "Bayesian network model for reliability assessment of power systems," *IEEE Transactions on Power Systems*, vol. 14, no. 2, pp. 426–432, May 1999.

[42] Yoh-Han Pao, *Adaptive Pattern Recognition and Neural Networks*, New York: John Wiley & Sons, Longman, 1989.

[43] R. O. Duda and P. E. Hart, *Pattern Classification and Scene Analysis*, New York: John Wiley & Sons, Jun. 1973.

[44] D. Shirmohammadi, P. R. Gribik, J. H. Malinowski and R. E. O'Donneell, "Evaluation of transmission network capacity use for wheeling transactions," *IEEE Transactions on Power Systems*, vol. 4, no. 4, pp. 1405-1413, Oct. 1989.

[45] D. Shirmohammadi, C. Rajagopalan, E. R. Alward and C. L. Thomas, "Cost of transmission transactions: An introduction," *IEEE Transactions on Power Systems*, vol. 6, no. 4, pp. 1546-1560, Nov. 1991.

[46] C.W. Yu and A. K. David, "Pricing transmission services in context of industry deregulation," *IEEE Transactions on Power Systems*, vol. 12, no. 1, pp. 1546-1560, Feb. 1997.

[47] E. L. Silva, S. E. C. Mesa and M. Morozowski, "Transmission access pricing to wheeling transactions: A reliability based approach," *IEEE Transactions on Power Systems*, vol. 13, no. 4, pp. 1481-1148, Nov. 1998.

[48] C.W. Yu and A. K. David, "Pricing reactive power conveyance," *in IEE Proceeding Generation, Transmission and Distribution, Part C,* vol. 140, no. 3, pp. 174-180, May 1993.

[49] L. K. Jr. Ford and D. K. Fulkerson, *Flows in Networks*, Princeton, NJ: Princeton University Press, 1962.

VITA

Hyungchul Kim was born in Pusan, Republic of Korea, on September 30, 1967. He received his Bachelor of Science degree in electrical engineering from the Korea University in February 1991. He continued his studies as an electrical engineering graduate student and research assistant in Korea University and received the Master of Science degree in February 1993. He then worked as a research engineer at LG Electronics Company for six years, where his main duties were hardware and software design for commercial products. Since August 1999, he has been with Texas A&M University, working towards his Doctor of Philosophy degree in electrical engineering. During his Ph.D. program, he worked as Graduate Research Assistant under guidance of Dr. Singh. His research area is power system reliability including power system security analysis and transmission pricing service. He is a student member of IEEE, the IEEE Power Engineering Society.

His permanent address is:

Hyungchul Kim
8-401 Woosung Apt. Bockchun-dong
Dongrae- Gu, Pusan, 607-751
Republic of Korea